Neutrophil Gelatinase-Associated Lipocalin From Macrophages Plays a Critical Role in Renal Fibrosis Via the CCL5 (Chemokine Ligand 5)-Th2 Cells-IL4 (Interleukin 4) Pathway

Benjamin Bonnard, Jaime Ibarrola, Ixchel Lima-Posada, Amaya Fernández-Celis, Manon Durand, Marie Genty, Natalia Lopez-Andrés, Frédéric Jaisser

Neutrophil Gelatinase-Associated Lipocalin from macrophages plays a critical role in renal fibrosis via the CCL5-Th2 cells-IL4 pathway.

Short title : NGAL macrophage role in renal fibrosis

Benjamin Bonnard[1] PhD, Jaime Ibarrola[2] PhD, Ixchel Lima-Posada[1] PhD, Amaya Fernández-Celis[2], Manon Durand[1] PhD, Marie Genty[1] MsC, Natalia López-Andrés[2] PhD, and Frédéric Jaisser[1,3] MD, PhD.

[1]Centre de Recherche des Cordeliers, INSERM, Sorbonne Université, Université de Paris, F-75006 Paris, France.

[2] Cardiovascular Translational Research, Navarrabiomed (Miguel Servet Foundation), Instituto de Investigación Sanitaria de Navarra (IdiSNA), Pamplona, Spain.

[3] INSERM, Clinical Investigation Centre 1433, French-Clinical Research Infrastructure Network (F-CRIN) INI-CRCT, Nancy, France.

Abstract

Neutrophil gelatinase-associated lipocalin (NGAL) (or lipocalin 2, Lcn2) is a novel mineralocorticoid target in the cardiovascular system. We showed that Lcn2 gene invalidation protects against proteinuria and renal injury upon mineralocorticoid excess and we hypothesized that NGAL produced from macrophages promotes the expression of chemoattractant molecules involved these renal lesions. The role of NGAL was analyzed using myeloid-specific (MΦ KO NGAL) Lcn2 knockout mice challenged with uni-nephrectomy, aldosterone, and salt (NAS) for six weeks. The role of the chemokine ligand 5 (CCL5) and interleukin 4 (IL4) in kidney fibrosis was studied by administration of the CCL5 receptor antagonist maraviroc or by injections of an anti-IL4 neutralizing antibody. In CTL mice, NAS increased the renal expression of extracellular matrix proteins, such as collagen I, αSMA, and fibronectin associated with interstitial fibrosis which were blunted in MΦ KO NGAL mice. The expression of CCL5 was blunted in sorted macrophages from MΦ KO NGAL mice challenged by NAS and in macrophages obtained from KO NGAL mice and challenged ex vivo with aldosterone and salt. The pharmacological blockade of the CCL5 receptor reduced renal fibrosis and the $CD4^+$ Th cell infiltration induced by NAS. Neutralization of IL4 in NAS mice blunted kidney fibrosis and the overexpression of profibrotic proteins, such as collagen I, αSMA, and fibronectin. In conclusion NGAL produced by macrophages plays a critical role in renal fibrosis and modulates the CCL5/IL4 pathway in mice exposed to mineralocorticoid excess.

Keywords: NGAL-macrophages-renal fibrosis-CCL5-IL4-aldosterone

Introduction

Aldosterone is a key regulator of blood pressure and electrolyte homeostasis via activation of the mineralocorticoid receptor (MR)[1]. Both animal models and clinical studies suggest that MR activation plays an important pathophysiological role in renal remodeling and inflammation[2,3], leading to organ failure. However, the precise mechanism by which MR activation leads to renal damage is still unclear. We previously identified neutrophil gelatinase–associated lipocalin (NGAL, also known as 24p3, siderocalin, and lipocalin 2) as a novel MR target in the cardiovascular system[4]. NGAL is a 25-kDa glycoprotein of the lipocalin superfamily[5] expressed by a variety of cell types, including renal cells[6], endothelial cells[7,8], smooth muscle cells[8], cardiomyocytes[4], and various immune-cell populations, such as neutrophils[9], macrophages[8,10], and dendritic cells[11]. We recently reported that NGAL expressed by myeloid cells[12], more specifically dendritic cells[13], is required for aldosterone-induced cardiac remodeling. NGAL is well recognized as a potent biomarker of renal injury[14] but it may also have a direct pathogenic role in renal disease. The involvement of immune cells in the mediation of renal injuries[15,16] is now well described, but the mechanism of action of NGAL in inflammatory cells has not yet been addressed in this context. We therefore hypothesized that NGAL is required for immune-cell recruitment and function, leading to renal damage induced by mineralocorticoid excess.

Here, we demonstrate the critical role of NGAL expressed in macrophages in aldosterone-induced renal injury using mice deficient for NGAL/lipocalin2. Moreover, we show that CCL5, a chemoattractant protein produced by macrophages, is involved in an underlying mechanism that links aldosterone, NGAL, immune cells, and renal fibrosis. These data support the potential therapeutic interest of modulating NGAL expression/activity to limit renal fibrosis.

MATERIALS & METHODS

A detailed Methods section is provided in the supplemental method. The data that support the findings of this study are available from the corresponding author upon reasonable request.

Institutional Review Board Statement

All animal studies were conducted in accordance with the National Institutes of Health Guide and European Community directives for the Care and Use of Laboratory Animals (European Directive, 2010/63/UE), approved by the local animal ethics committee (APAFIS#7420-2016102718076839) and conducted according to the INSERM animal care and use committee guidelines.

Mice

Animals were housed in a climate-controlled facility with a 12-h/12-h light/dark cycle and provided free access to food (A04, Safediets; Augy, France) and water.

The specific inaction of Lcn2 gene in myeloid cells was generated by crossing Lcn2 floxed mice (Jackson Laboratory) with transgenic mice expressing the Cre recombinase under the control of the LysM promoter (The Jackson Laboratory, Bar Harbor, ME)[17]. From this breeding, Cre positive pups were selected as MΦ KO NGAL and Cre negative pups as control (MΦ CTL). Commercial C57BL6 mice from Charles Rivers Laboratory (Saint Germain Nuelles, France) were used. The NAS model was produced in eight-week-old mice with uni-nephrectomy, osmotic minipumps (Charles River Laboratory, model 1004 and 2006 for respectively 8 days and 6 weeks treatment) delivering aldosterone (200 µg/kg/d, Sigma-Aldrich) implanted subcutaneously in treated animals, and drinking water supplemented with 1% NaCl (Sigma-Aldrich) (NAS). All mice were maintained on normal chow and sacrificed either eight days or six weeks later. To inhibit CCL5 signaling, mice were treated with Maraviroc (MARA; ViiV Healthcare), a CCL5 receptor antagonist, incorporated into normal chow (A04) at a dose of 312.5 mg/kg chow to achieve a daily dose of 50 mg/kg for six weeks. To interfere with IL4 signaling, mice received intraperitoneal injections of 200 µg rat anti-mouse IL4 antibody (diluted in 200 µl PBS) (Clone 11B11; BioXCell) three times per week for six weeks. Rat IgG1 (Clone TNP6A7; BioXCell) was used as a control. Anti-mouse IL4 antibody and its IgG1control were diluted in saline solution (ThermoFisher) to inject 200 µl per mouse.

Flow cytometry and sorted cells

Kidney cells were obtained using the gentle MACS dissociation kit (Miltenyi Biotec) following the provider's instructions. For intracellular staining, half of the cells were co-treated with PMA (50 ng/ml, Sigma-Aldrich) and ionomycin (100 ng/ml, Sigma-Aldrich) in the presence of brefeldin A (5 µg/ml, BioLegend) for 4 h at 37°C. Fc receptors were blocked with Fc Block (1/100, BD Bioscience) for 5 min and the cells incubated for 30 min with an antibody cocktail which included, PE-CF594 anti-mouse CD45 (1/1000), BV510 anti-mouse Ly6C (1/100), BV650 anti-mouse CD19 (1/200), PE anti-mouse CD3 (1/100), APC/Cy7 anti-mouse CD11b (1/300), PE/Cy7 anti-mouse F4/80 (1/200), APC anti-mouse CD8 (1/200), PerCP anti-mouse CD4 (1/200), and FITC anti-mouse CD206 (1/100), all from BioLegend. Cells were permeabilized with Cytofix/Cytoperm (BD Bioscience) and then exposed to A888 anti-mouse IL4 (BioLegend, 1/100). Unstimulated cells were blocked and then stained with specific antibodies against the extracellular targets (see above). Cells were sorted using an Aria II cytometer (BD Bioscience) and immune populations analyzed using an LFR Fortessa (Becton

Dickinson) cytometer. Recorded data were analyzed using FlowJo V10.7 software (BD Bioscience). The absolute counts (cells/mg of kidney) were performed to analyze the cell infiltration and mean fluorescent intensity (MFI) was recorded for IL4 expression. The gating strategy is presented in Figure S1A-E.

Statistics

All analyses were performed using GraphPad Prism V6.01 (GraphPad Software, San Diego, CA) software. The two-tailed significance level was set to $P < 0.05$. Results are expressed as the mean ± SEM. Data were analyzed by two-way ANOVA followed by Tukey's multiple comparisons test (two groups and two treatments) or one-way ANOVA followed by Tukey's multiple comparisons test (more than two conditions) or unpaired t tests (two groups). Differential expression of gene expression obtained by NanoString analysis was determined using false discovery change two-stage step-up method for Benjamini, Krieger and Yekutieli.

RESULTS

NGAL inactivation in macrophages blunts mineralocorticoid-induced kidney fibrosis

As shown by others[18], we demonstrated that global depletion of NGAL prevented kidney injury induced by mineralocorticoid excess. Briefly, NAS challenge of WT mice (WT NAS) for six weeks induced an increase of systolic blood pressure (SBP) relative to untreated mice (WT CONTROL) and kidney hypertrophy (Table S1). NAS challenge induced renal dysfunction, leading to an increase in plasma creatinine levels in WT NAS mice relative to WT CONTROL mice (Table S1). Global NGAL gene inactivation prevented the rise of SBP and creatinine levels induced by NAS challenge (KO NGAL NAS *vs* WT NAS) (Table S1). WT NAS mice showed higher levels of renal interstitial fibrosis associated with high expression level of protein involved in tissue remodeling (such as collagen I, fibronectin, and αSMA) than WT mice (Figure S2A-B). These increases were fully prevented in KO NGAL mice (Figure S2A-B). The analysis of renal inflammation revealed that NAS increased gene expression of proinflammatory genes such as *IL1β*, *IL6*, *TNFα, MCP1,* and *CCL5* in whole kidney from WT mice (Figure S2C). These modifications were partly (*IL6*, *TNFα* and *MCP1*) or fully prevented (*CCL5*) in KO NGAL mice (Figure S2C). FACS analysis revealed that the NAS challenge leads to renal infiltration by $CD11b^{+}$ $F4/80^{high}$ cells that refers to mature macrophages[19] (Figure S2D) with an increase of NGAL gene expression in macrophages (2.86-fold, $P < 0.05$ vs WT CONTROL, n=5. Total NGAL depletion prevents $CD11b^{+}$ $F4/80^{high}$ cell infiltration induced by NAS in KO NGAL mice (Figure S2D). To discriminate between acute and long term effects

and possible subsequent adaptation, we analyzed mice exposed to a short NAS challenge (8 days). We showed that CD11b^{+} F4/80^{high} cells isolated from the kidney of KO NGAL mice challenged with NAS presented lower gene expression for several proinflammatory cytokines and chemokines, such as *IL1β*, *TNFα, MCP1,* and *CCL5* (Figure S2E). The data pointed out a possible role of NGAL expressed in immune cells in kidney injury.

To assess the role of NGAL originating from myeloid cells in vivo, we generated a model with NGAL inactivation in myeloid cells by bone marrow transfer. This resulted in mice with NGAL inactivation in myeloid cells only (KO BM) and their control mice without NGAL deletion in myeloid cells (WT BM), as we previously reported[12]. The increase in systolic blood pressure induced by NAS in WT BM mice was partly blunted in KO BM mice but remained higher than in WT BM mice (Figure S3B). WT BM mice subjected to NAS challenge showed increased renal interstitial fibrosis (Figure S3C), an effect partly blunted in KO BM mice (Figure S3C) suggesting a role of NGAL expressed in myeloid cells.

To assess the specific role of NGAL expressed in myeloid cells, we next analyzed the consequences of macrophage deletion of NGAL upon NAS challenge using a mouse model with myeloid-specific NGAL deletion (MΦ KO NGAL) confirmed by the absent NGAL gene expression in sorted MΦ KO NGAL macrophages (CD11b^{+} F4/80^{high}) (Figure S4). The chronic NAS challenge induced kidney hypertrophy and increased plasma creatinine levels relative to the control group (MΦ CTL NAS *vs* MΦ CTL CONTROL) (Table 1). These effects were not prevented in MΦ KO NGAL mice. The increased blood pressure observed in NAS mice was partly blunted in MΦ KO NGAL but remain higher than in MΦ CTL mice (Table 1). The increase of renal interstitial fibrosis and the expression of collagen I, fibronectin, and αSMA induced by NAS was blunted but no fully prevented in MΦ KO NGAL mice (Figure 1A-B), similarly to what we observed in KO BM mice (Figure S3C). The increase of various proinflammatory markers by NAS was blunted in MΦ KO NGAL mice for *TNFα, MCP1* and *CCL5* while expression of *IL1β* and *IL6* was unchanged (Figure 1C). The renal phenotyping of untreated MΦ WT and MΦ KO NGAL mice revealed no differences between groups (Figure S5A-C). SBP (mmHg, ± SEM; MΦ CTL: 102.3 ± 1.73; MΦ KO NGAL 106.6 ± 1.09, P>0.05, n=8) and plasma creatinine levels (μM, mean ± SEM, MΦ CTL: 11.1 ± 0.96 ; MΦ KO NGAL 10.5 ± 0.99, P>0.05, n=8) are similar between untreated MΦ CTL and MΦ KO NGAL mice.

The flow cytometry analyses revealed that CD11b^{+} F4/80^{high} cell infiltration induced by NAS is unchanged in MΦ KO NGAL mice (Figure 1D), at difference with the global KO NGAL

mice (Figure S2D). Interestingly, macrophages isolated from MΦ KO NGAL mice exposed to short-term (8 days) NAS showed decreased expression of *IL1β*, *TNFα, MCP1,* and *CCL5* (Figure 1E) suggesting a direct role of NGAL expressed in macrophages on cytokine/chemokine expression *in vivo*.

Taken together, these results suggest a role of NGAL produced by macrophages in aldosterone-induced in renal interstitial fibrosis.

NGAL is required for proinflammatory cytokine/chemokine expression in macrophages upon ex vivo aldosterone stimulation

The role of macrophages in aldosterone-induced renal lesions has been reported and macrophage depletion blunted interstitial renal fibrosis upon aldosterone challenge in rats[20]. Since we previously showed that NGAL expression is induced in macrophages isolated from mice challenged by NAS[12], we therefore analyzed whether NGAL impacts macrophages upon mineralocorticoid challenge. Peritoneal macrophages from WT (WT MΦ) and KO NGAL mice (KO NGAL MΦ) were isolated then co-treated with aldosterone and salt (A/S). NGAL gene expression was induced by A/S (2.52-fold, $P < 0.0001$ vs CONTROL, n=5). Gene expression profiling using NanoString technology showed 27 downregulated and 4 upregulated genes in KO NGAL MΦ + A/S versus WT MΦ + A/S (Figure 2A), mainly involved in inflammatory response (detailed gene list is provided in Table S2). Gene expression analysis of proinflammatory markers confirmed that A/S induced the expression of *IL1β*, *IL6*, *TNFα, MCP1,* and *CCL5* (Figure 2B). Importantly genetic deletion of NGAL blunted the induction of *IL6* and *CCL5* expression by A/S in peritoneal KO NGAL MΦ (Figure 2B). Of note, aldosterone or salt alone treatment did not modify CCL5 gene expression in cultured WT MΦ (Figure S6). We also showed that recombinant NGAL treatment on KO NGAL MΦ exposed to A/S treatment (KO NGAL MΦ + A/S + recNGAL) rescued the increase of CCL5 expression compared to KO NGAL MΦ + A/S (1.76-fold, $P < 0.05$, vs KO NGAL MΦ + A/S, n=8). Indeed CCL5 is the only proinflammatory chemokine for which the induction was prevented in the various *in vivo* and *in vitro* models used in this study. Furthermore, CCL5 has been previously shown to be involved in renal fibrosis[21,22]. We therefore hypothesized that CCL5 may be a key NGAL-modulated mediator of the renal pro-fibrotic effects of aldosterone-salt challenge.

Pharmacological CCL5 receptor antagonism blunts NAS-induced renal fibrosis

We assessed the pathogenic role of CCL5 in the NAS challenge by subjecting C57BL6 WT mice to NAS challenge with or without administration of Maraviroc, a CCL5 receptor (CCR5) antagonist. NAS induced kidney hypertrophy, higher SBP, and an increase in plasma creatinine levels relative to the control group (Table 1). Maraviroc (NAS + MARA) did not alter these changes (Table 1). However Maraviroc treatment blunted the renal fibrosis induced by NAS (Figure 3A) and prevented the increased expression of several pro-fibrotic markers (collagen I, fibronectin, and αSMA) (Figure 3B). Maraviroc did not reduce NAS-induced gene expression of pro-inflammatory markers (*IL1β, IL6, TNFα*, *MCP1*, or *CCL5*), suggesting that it acts downstream of these pathways (Figure 3C).

Overall, these data showed that CCL5 is involved in kidney fibrosis induced by mineralocorticoid excess and contributes to the NGAL-mineralocorticoid profibrotic effect.

CCL5 mediates T-cell recruitment in NAS-induced renal damage

CCL5 is one of several secreted chemokines that play a key role in T-cell recruitment to inflamed areas. T cells are immune cells that are involved in adaptive immunity and it is known that T-cell infiltration is associated with renal fibrosis[23]. T cells can be subdivided into several subsets with various physiological functions. $CD4^+$ T helper cells (Th) play a crucial role in adaptive immune responses and can be split into several subsets. Two major subsets are IFNγ-producing Th1 cells and IL4-producing Th2 cells. These two T-cell subsets have opposite roles in extracellular matrix remodeling, as Th1 cells are involved in collagen degradation, whereas Th2 cells enhance collagen deposition[24]. mRNA expression analysis of T cells markers revealed that NAS challenge increased expression of CD3, CD8, CD4 mRNAs associated with an increase of IL4 mRNA expression (Figure S7A-C) while *IFNγ* expression is unchanged by NAS challenge (Figure S7A-C), suggesting that Th2 cells are important in this context. This NAS-induced gene overexpression was limited by global or specific inhibition of NGAL expression in macrophages and MARA treatment (Figure S7A-C).

FACS analysis indicated that NAS induced an increase in renal Th cells ($CD3^+$ $CD4^+$) infiltration (Figure 4A) associated with an increase of IL4 protein expression in $CD3^+$ $CD4^+$ population (Figure 4B) indicating an increase in renal Th2 cells. We showed that *IL4* expression is positively correlated with *CD4* expression in kidney from mice exposed to NAS challenge in our different models (Figure S8A). The NAS-induced CD4 gene expression is blunted in NAS + MARA group (Figure S8B-C). The gene expression of IL4 also increased following NAS challenge, an effect blunted in the NAS + MARA mice (Figure 4C) and fully prevented in the

MΦ KO NGAL mice (Figure 4D). $CD3^+$ $CD4^+$ infiltration and IL4 expression is lower in NAS-treated MΦ KO NGAL mice compared to NAS-treated MΦ CTL mice (Figure S9 and Figure 4D) suggesting that NGAL expressed by macrophages is involved in Th2 cell infiltration.
Overall, these results reveal a role for CCL5 in NAS-induced renal lesions and the benefit of macrophage NGAL deletion in blunting CCL5-mediated Th cells recruitment associated with reduced IL4 expression. These results suggest that IL4 secreted by Th2 cells participates to mineralocorticoid-induced fibrosis mediated by the NGAL/CCL5 signaling pathway.

IL4 is involved in the renal profibrotic effects of NAS

We assessed whether IL4 has a direct pro-fibrotic role in mouse kidney fibroblasts (MKFs). Recombinant IL4 treatment induced an increase in STAT6 phosphorylation in MKFs relative to the control group (Figure 5A), associated with increased expression of genes involved in ECM remodeling (*collagen I*, *collagen IV*, *αSMA,* and *fibronectin*) relative to that in untreated cells (Figure 5B). The secretion of collagen I into the supernatant of MKFs cells is increased upon recombinant IL4 stimulation (Figure S10). Co-treatment with IL4 and a STAT6 inhibitor (IL4 + STAT6i) prevented these modifications (Figure 5A-B and Figure S10).
We next tested whether IL4 is primarily involved *in vivo* in the NAS-induced renal fibrosis by challenging C57BL6 mice with NAS and treating them with an anti-IL4 neutralizing antibody (NAS + IL4 AB) or an IgG1 isotype control antibody (NAS + IgG1). NAS challenge induced kidney hypertrophy, higher SBP, and renal dysfunction in both groups (Table 1). Interstitial fibrosis was blunted in the NAS + IL4 AB mice relative to NAS mice treated with the IgG1 isotype (Figure 5C). The analysis of proteins involved in extracellular matrix remodeling (collagen I and fibronectin) confirmed the anti-fibrotic effect of the anti-IL4 antibody on NAS-induced renal lesions (Figure 5D). Anti-IL4 antibody administration had no effect on NAS - induced gene expression of pro-inflammatory markers (*IL1β, IL6, TNFα*, *MCP1* and *CCL5*) (Figure S11). These results showed that IL4 contributes to the development of renal fibrosis mediated by the aldosterone/NGAL/CCL5 signaling pathway.

Discussion

NGAL is a well-recognized biomarker of renal injury but a role for NGAL as a mediator of renal injury has also been proposed.[25,26] Mice with an NGAL deletion are protected from glomerulosclerosis and interstitial fibrosis in a CKD model with nephron reduction[25] and in proteinuria models[26]. Administration of recombinant NGAL induces chronic renal injury in

mice lacking endogenous NGAL expression[18]. NGAL is a predictor of poor prognosis in patients with renal failure and elevated NGAL levels are associated with renal damage in CKD patients[27], while patients with high NGAL levels have an increased risk of CKD progression[28]. This is not restricted to the renal field, as elevated serum NGAL levels have been reported to be a marker of poor prognosis for patients with acute myocardial infarction, heart failure, and stroke[29]. We and others have accumulated preclinical data suggesting a broader pathogenic role for NGAL in cardiovascular (CV) diseases[8,30–36], indicating that NGAL is more than a simple biomarker and could be a potential therapeutic target in cardiorenal diseases[37]. This suggests a direct pathogenic role for NGAL in the progression of renal diseases but the exact pathogenic mechanisms are yet to be established.

We previously showed that NGAL is indeed an aldosterone/MR target. In the presence of aldosterone, MR binds to the -794 to +36 NGAL promoter and modulates promoter activity[4]. NGAL expression is dose-dependently modulated by aldosterone in cardiac cells and pharmacological MR blockade blunts NGAL expression, both ex vivo in cultured cells and in vivo upon aldosterone challenge[4]. Aldo/MR-dependent expression of NGAL has also been reported by others in the vasculature , adipose tissue[18], and human neutrophils[39]. NGAL is able to form a disulfide bridge with matrix metalloproteinase-9 (MMP9) avoiding his degradation[40]. The co-expression of NGAL and MMP9 has been showed is CV diseases such as atherosclerosis[41], cerebrovascular ischemia[42] and abdominal aortic aneurysm (AAA)[43]. We already reported the positive correlation between high plasma level of NGAL/MMP9 complex and circulating fibrosis markers in obese patients[44]. In a mouse AAA model, NGAL inhibition has a protective effect associated with decrease of MMP activity[45]. In patients with metabolic disease, a plasma NGAL-MMP9 complex is associated with plasma aldosterone levels[30], while urinary NGAL is associated with urinary aldosterone levels[46].

In the present study we determined a key role of NGAL produced by macrophages and of the downstream signaling though the CCL5-Th2 cells-IL4 pathway in the development of renal fibrosis induced by mineralocorticoid excess. While the full NGAL deletion fully prevented NAS-induced fibrosis, the BMT experiments and the macrophage-targeted NGAL deletion only blunted interstitial fibrosis suggesting that non-inflammatory sources of NGAL are also important. A recent study reported that NGAL originating from adipocytes blunted the impact of NAS on kidney injury, highlighting an important role for adipocyte production of NGAL in driving renal injury[18].

The role of immune cells in hypertensive,[47,48] cardiac[49], and renal[15] diseases is now very-well documented. Recent studies have demonstrated the involvement of the MR of immune cells in these diseases.[50–53] Specific production of NGAL by immune cells plays an important role in the mediation of mineralocorticoid-induced hypertension, cardiac remodeling and cardiac injuries. We previously reported that NAS challenge induces the recruitment of various populations of immune cells to the lymph nodes, highlighting the pro-inflammatory role of aldosterone: NAS challenge induces increased NGAL expression in MΦ, PBMCs, and DCs, revealing a role for aldosterone in NGAL production by these immune-cell populations[12]. We also reported that myeloid-cell deletion of NGAL using BMT blunted the cardiac extracellular matrix remodeling induced by NAS[12].

Here, we showed that NGAL creates a pro-inflammatory environment (shown by increased expression of the pro-inflammatory markers MCP1, IL6, TNFα, and CCL5) that leads to the recruitment of further inflammatory cells to the kidney, therefore promoting organ damage. This finding is consistent with previous reports highlighting a role for NGAL in the recruitment of immune cells to sites of inflammation. For example, Aigner *et al.* showed that immune-cell recruitment to the hearts of mice subjected to ischemia-reperfusion (IR) is significantly prevented in KO NGAL mice.[54] Impaired recruitment of immune cells in KO NGAL mice has been associated with reduced levels of chemokines that promote infiltration[55] and adhesion of pro-inflammatory cells[56]. Finally, NGAL neutralization using mouse anti-NGAL monoclonal antibodies decreases the recruitment of MΦ after myocardial IR injury and suppresses local expression of various pro-inflammatory markers[39].

NGAL is expressed in various immune cells upon NAS challenge[12,13]. We recently reported that NGAL expressed in dendritic cells, while being required for cardiac remodeling induced by a mineralocorticoid challenge, has no effect on kidney fibrosis and inflammation[13]. NGAL expressed in macrophages is important for macrophage polarization[36,57]. Indeed NGAL inhibition prevented LPS-induced macrophage M1 polarization and enhanced IL10-induced macrophage M2 polarization[36]. We recently showed the direct effect of recombinant NGAL to prevent the phenotype switch from M1 to M2 macrophage[57].In another context, Ye et al. showed in a mouse NASH model that NGAL expressed by bone marrow cells is involved in macrophages and neutrophil infiltration in liver[58]. Furthermore, they revealed that NGAL enhances neutrophil migration through CXCR2 signaling[58].

Macrophages have been shown to be important mediators of mineralocorticoid-induced organ damage[59]. We therefore assessed the impact of aldosterone-salt on peritoneal macrophages and identified CCL5 as a macrophage aldosterone target, of which the expression is dependent on NGAL expression in macrophages. Of note, CCL5 has been previously reported to be a mineralocorticoid-modulated cytokine in a several organs, including the kidney[60,61]. CCL5 has been reported to be involved in renal injury in a variety of pathological settings, such as acute renal failure, renal obstruction, chronic kidney disease, diabetic nephropathy, and chronic kidney disease[62]. A direct profibrotic effect of CCL5 has been reported using a pharmacological CCL5 receptor (CCR5) antagonist or an anti-CCL5 neutralizing antibody [21,22]. However, the absence of a protective effect in CCL5 knock-out mice upon DOCA + Angiotensin II challenge has also been reported[63]. Of note the CCR5 antagonist used in the present study and by Lefebvre E *et al*.[22] also inhibit CCL3 and CCL4 signaling.

The role of $CD4^+$ Th2 cells in renal fibrosis is still controversial. Shapell *et al.* reported that $CD4^+$ Th cells do not contribute to renal damage in a model of chronic obstructive uropathy[64]. However, two other groups showed a role of $CD4^+$ Th cells, especially the Th2 subset, in the development of renal fibrosis[65,66]. Th2 cells are major source of IL4 but other immune cells could produce IL4 such as B cells, mast cells, basophils and eosinophils[67]. Previous studies showed that the deletion of IL4 receptor α (IL4Rα) in bone marrow-derived fibroblasts (BMDF) protects against renal fibrosis in folic acid and unilateral ureteral obstruction (UUO) models[68]. JAK3/STAT6 signaling (downstream of IL4) has been shown to be involved in UUO-induced renal fibrosis[69]. IL4 has been reported as a profibrotic interleukin outside of the kidney: in CCL4-induced liver fibrosis, the loss of IL4Rα protects against liver inflammation and the progression of fibrosis and the administration of an anti-IL4 neutralizing antibody also prevents the development of dermal fibrosis in a model of systemic sclerosis[71]. A direct pro-fibrotic role for IL4 has been reported in cardiac remodeling in IL4 KO mice treated with angiotensin II[72], whereas administration of an anti-IL4 neutralizing antibody in a model of cardiac pressure overload prevented cardiac fibrosis[73], similarly to what we report here for the kidney. Of interest, a correlation between urinary IL4 levels and cardiac fibrosis has been shown in patients with heart failure[74]. This measurement has not been performed in CKD patients, but our study suggests a pivotal role for IL4 in the progression of renal fibrosis.

Perspectives

In summary, our study shows that NGAL is an important mediator of aldosterone-induced renal damage through pro-inflammatory and pro-fibrotic mechanisms. Our current mechanistic scheme (Figure S12) is that mineralocorticoid-salt induced NGAL expression in macrophages leads to CCL5 expression and subsequent Th2 cell infiltration and IL4-associated renal interstitial fibrosis. The role of NGAL in CKD progression and in CV diseases is now well established and NGAL is a potential therapeutic target. Recently, we described an antifibrotic effect of a new NGAL inhibitor in cardiac and renal disease models[75]. In the present study, renal fibrosis induced by mineralocorticoid excess was not fully prevented by the specific depletion of NGAL in macrophages suggesting that others sources of NGAL could be involved in fibrosis development and this should be assessed in future studies.

Novelty and significance

What is new?

- Specific NGAL-deletion in macrophages blunts proinflammatory cytokines and chemokines overexpression induced by mineralocorticoid challenge limiting renal remodeling and inflammation

Why is it relevant?

- We described a novel NGAL signaling pathway through CCL5-Th cells-IL4 that could be targeted in hypertension-induced end-organ damage.

Summary

The deleterious role of NGAL in renal injury induced by mineralocorticoid excess is now established but identifying the source of NGAL involved in renal remodeling is more challenging. We showed that NGAL macrophage through the CCL5-Th cells-IL4 pathway participates to renal fibrosis induced by mineralocorticoid excess.

Author contributions

F.J and N.A designed the study. B.B, J.I, I.L.P, M.D, A.F.C, and M.G carried out the experiments. B.B analyzed the data. B.B and A.F.C made the figures. B.B, N.A, and F.J drafted and revised the paper. All authors approved the final version of the manuscript.

Disclosure

The authors have no conflict of interest to declare.

Funding

This work was funded by grants from the Institut National de la Santé et de la Recherche Médicale, the Fight-HF Avenir investment program (ANR-15-RHUS-0004), the Fondation de Recherche sur l'Hypertension Artérielle (REIN/NgalPA - 2017/2018), the ANR NGAL-HT (ANR-19-CE14-0013). NL-A was supported by a Miguel Servet contract CP13/00221 from the "Instituto de Salud Carlos III-FEDER". BB was supported by a PhD grant from the Region Ile de France ArDoc.

Acknowledgments

We thank the team of the CEF of the Cordeliers Research Center for their support with animal care. We also thank Dr. We are grateful to Thorsten Berger and Tak W. Mak (University of Toronto, Canada) for kindly sharing the NGAL KO mice and to E. Martinez-Martinez and M. Buonafine their input in the BMT studies. Flow cytometry analysis was performed at the Centre d'Imagerie Cellulaire et de Cytométrie (CICC).

References

1. Rogerson FM, Fuller PJ. Mineralocorticoid action. *Steroids*. 2000;65(2):61-73.

2. Briet M, Schiffrin EL. Aldosterone: effects on the kidney and cardiovascular system. *Nat Rev Nephrol*. 2010;6(5):261-273. doi:10.1038/nrneph.2010.30

3. Cachofeiro V, Miana M, de las Heras N, et al. Aldosterone and the vascular system. *J Steroid Biochem Mol Biol*. 2008;109(3-5):331-335. doi:10.1016/j.jsbmb.2008.03.005

4. Latouche C, El Moghrabi S, Messaoudi S, et al. Neutrophil gelatinase-associated lipocalin is a novel mineralocorticoid target in the cardiovascular system. *Hypertension*. 2012;59(5):966-972. doi:10.1161/HYPERTENSIONAHA.111.187872

5. Schmidt-Ott KM, Mori K, Li JY, et al. Dual Action of Neutrophil Gelatinase-Associated Lipocalin. *J Am Soc Nephrol*. 2007;18(2):407-413. doi:10.1681/ASN.2006080882

6. Liu F, Yang H, Chen H, Zhang M, Ma Q. High expression of neutrophil gelatinase-

associated lipocalin (NGAL) in the kidney proximal tubules of diabetic rats. *Adv Med Sci*. 2015;60(1):133-138. doi:10.1016/j.advms.2015.01.001

7. Hamzic N, Blomqvist A, Nilsberth C. Immune-Induced Expression of Lipocalin-2 in Brain Endothelial Cells: Relationship with Interleukin-6, Cyclooxygenase-2 and the Febrile Response. *J Neuroendocrinol*. 2013;25(3):271-280. doi:10.1111/jne.12000

8. Eilenberg W, Stojkovic S, Piechota-Polanczyk A, et al. Neutrophil Gelatinase-Associated Lipocalin (NGAL) is Associated with Symptomatic Carotid Atherosclerosis and Drives Pro-inflammatory State In Vitro. *Eur J Vasc Endovasc Surg*. 2016;51(5):623-631. doi:10.1016/j.ejvs.2016.01.009

9. Kjeldsen L, Johnsen AH, Sengelov H, Borregaard N. Isolation and primary structure of NGAL, a novel protein associated with human neutrophil gelatinase. *J Biol Chem*. 1993;268:10425-10432.

10. Flo TH, Smith KD, Sato S, et al. Lipocalin 2 mediates an innate immune response to bacterial infection by sequestrating iron. *Nature*. 2004;432(7019):917-921. doi:10.1038/nature03104

11. Floderer M, Prchal-Murphy M, Vizzardelli C. Dendritic Cell-Secreted Lipocalin2 Induces CD8+ T-Cell Apoptosis, Contributes to T-Cell Priming and Leads to a TH1 Phenotype. Appel S, ed. *PLoS ONE*. 2014;9(7):e101881. doi:10.1371/journal.pone.0101881

12. Buonafine M, Martínez-Martínez E, Amador C, et al. Neutrophil Gelatinase-Associated Lipocalin from immune cells is mandatory for aldosterone-induced cardiac remodeling and inflammation. *J Mol Cell Cardiol*. 2018;115:32-38. doi:10.1016/j.yjmcc.2017.12.011

13. Araos P, Prado C, Lozano M, et al. Dendritic cells are crucial for cardiovascular remodeling and modulate neutrophil gelatinase-associated lipocalin expression upon mineralocorticoid receptor activation. *J Hypertens*. 2019;Publish Ahead of Print. doi:10.1097/HJH.0000000000002067

14. Devarajan P. Neutrophil gelatinase-associated lipocalin: a promising biomarker for human acute kidney injury. *Biomark Med*. 2010;4(2):265-280. doi:10.2217/bmm.10.12

15. Imig JD, Ryan MJ. Immune and Inflammatory Role in Renal Disease. In: Terjung R, ed. *Comprehensive Physiology*. John Wiley & Sons, Inc.; 2013. doi:10.1002/cphy.c120028

16. Montecucco F, Liberale L, Bonaventura A, Vecchiè A, Dallegri F, Carbone F. The Role of Inflammation in Cardiovascular Outcome. *Curr Atheroscler Rep*. 2017;19(3). doi:10.1007/s11883-017-0646-1

17. Clausen BE, Burkhardt C, Reith W, Renkawitz R, Förster I. Conditional gene

targeting in macrophages and granulocytes using LysMcre mice. *Transgenic Res*. 1999;8(4):265-277. doi:10.1023/A:1008942828960

18. Sun WY, Bai B, Luo C, et al. Lipocalin-2 derived from adipose tissue mediates aldosterone-induced renal injury. *JCI Insight*. 2018;3(17):120196. doi:10.1172/jci.insight.120196

19. Clements M, Gershenovich M, Chaber C, et al. Differential Ly6C Expression after Renal Ischemia-Reperfusion Identifies Unique Macrophage Populations. *J Am Soc Nephrol JASN*. 2016;27(1):159-170. doi:10.1681/ASN.2014111138

20. Martín-Fernández B, Rubio-Navarro A, Cortegano I, et al. Aldosterone Induces Renal Fibrosis and Inflammatory M1-Macrophage Subtype via Mineralocorticoid Receptor in Rats. *PloS One*. 2016;11(1):e0145946. doi:10.1371/journal.pone.0145946

21. Peng X, Xiao Z, Zhang J, Li Y, Dong Y, Du J. IL-17A produced by both γδ T and Th17 cells promotes renal fibrosis via RANTES-mediated leukocyte infiltration after renal obstruction. *J Pathol*. 2015;235(1):79-89. doi:10.1002/path.4430

22. Lefebvre E, Moyle G, Reshef R, et al. Antifibrotic Effects of the Dual CCR2/CCR5 Antagonist Cenicriviroc in Animal Models of Liver and Kidney Fibrosis. *PLoS ONE*. 2016;11(6). doi:10.1371/journal.pone.0158156

23. Strutz F, Neilson EG. The role of lymphocytes in the progression of interstitial disease. *Kidney Int Suppl*. 1994;45:S106-110.

24. Wynn TA. Fibrotic disease and the T H 1/T H 2 paradigm. *Nat Rev Immunol*. 2004;4(8):583-594. doi:10.1038/nri1412

25. Viau A, El Karoui K, Laouari D, et al. Lipocalin 2 is essential for chronic kidney disease progression in mice and humans. *J Clin Invest*. 2010;120(11):4065-4076. doi:10.1172/JCI42004

26. El Karoui K, Viau A, Dellis O, et al. Endoplasmic reticulum stress drives proteinuria-induced kidney lesions via Lipocalin 2. *Nat Commun*. 2016;7:10330. doi:10.1038/ncomms10330

27. Bolignano D, Lacquaniti A, Coppolino G, et al. Neutrophil gelatinase-associated lipocalin (NGAL) and progression of chronic kidney disease. *Clin J Am Soc Nephrol CJASN*. 2009;4(2):337-344. doi:10.2215/CJN.03530708

28. Bolignano D, Donato V, Coppolino G, et al. Neutrophil gelatinase-associated lipocalin (NGAL) as a marker of kidney damage. *Am J Kidney Dis Off J Natl Kidney Found*. 2008;52(3):595-605. doi:10.1053/j.ajkd.2008.01.020

29. Helanova K, Spinar J, Parenica J. Diagnostic and Prognostic Utility of Neutrophil

Gelatinase-Associated Lipocalin (NGAL) in Patients with Cardiovascular Diseases - Review. *Kidney Blood Press Res*. 2014;39(6):623-629. doi:10.1159/000368474

30. Tarjus A, Martínez-Martínez E, Amador C, et al. Neutrophil Gelatinase–Associated Lipocalin, a Novel Mineralocorticoid Biotarget, Mediates Vascular Profibrotic Effects of Mineralocorticoids. *Hypertension*. 2015;66(1):158-166. doi:10.1161/HYPERTENSIONAHA.115.05431

31. Yndestad A, Landrø L, Ueland T, et al. Increased systemic and myocardial expression of neutrophil gelatinase-associated lipocalin in clinical and experimental heart failure. *Eur Heart J*. 2009;30(10):1229-1236. doi:10.1093/eurheartj/ehp088

32. Yang B, Fan P, Xu A, et al. Improved functional recovery to I/R injury in hearts from lipocalin-2 deficiency mice: restoration of mitochondrial function and phospholipids remodeling. *Am J Transl Res*. Published online 2012. Accessed September 6, 2016. http://hub.hku.hk/handle/10722/159686

33. Tarín C, Fernandez-Garcia CE, Burillo E, et al. Lipocalin-2 deficiency or blockade protects against aortic abdominal aneurysm development in mice. *Cardiovasc Res*. 2016;111(3):262-273. doi:10.1093/cvr/cvw112

34. Hemdahl A-L. Expression of Neutrophil Gelatinase-Associated Lipocalin in Atherosclerosis and Myocardial Infarction. *Arterioscler Thromb Vasc Biol*. 2006;26(1):136-142. doi:10.1161/01.ATV.0000193567.88685.f4

35. Sung HK, Chan YK, Han M, et al. Lipocalin-2 (NGAL) Attenuates Autophagy to Exacerbate Cardiac Apoptosis Induced by Myocardial Ischemia: LIPOCALIN-2, AUTOPHAGY AND CELL DEATH. *J Cell Physiol*. Published online March 2017. doi:10.1002/jcp.25672

36. Cheng L, Xing H, Mao X, Li L, Li X, Li Q. Lipocalin-2 Promotes M1 Macrophages Polarization in a Mouse Cardiac Ischaemia–Reperfusion Injury Model. *Scand J Immunol*. 2015;81(1):31-38. doi:10.1111/sji.12245

37. Buonafine M, Martinez-Martinez E, Jaisser F. More than a simple biomarker: the role of NGAL in cardiovascular and renal diseases. *Clin Sci Lond Engl 1979*. 2018;132(9):909-923. doi:10.1042/CS20171592

38. Amador CA, Bertocchio J-P, Andre-Gregoire G, et al. Deletion of mineralocorticoid receptors in smooth muscle cells blunts renal vascular resistance following acute cyclosporine administration. *Kidney Int*. 2016;89(2):354-362. doi:10.1038/ki.2015.312

39. Gilet A, Zou F, Boumenir M, et al. Aldosterone up-regulates MMP-9 and MMP-9/NGAL expression in human neutrophils through p38, ERK1/2 and PI3K pathways. *Exp Cell*

Res. 2015;331(1):152-163. doi:10.1016/j.yexcr.2014.11.004

40. Yan L, Borregaard N, Kjeldsen L, Moses MA. The high molecular weight urinary matrix metalloproteinase (MMP) activity is a complex of gelatinase B/MMP-9 and neutrophil gelatinase-associated lipocalin (NGAL). Modulation of MMP-9 activity by NGAL. *J Biol Chem*. 2001;276(40):37258-37265. doi:10.1074/jbc.M106089200

41. Soylu K, Nar G, Aksan G, et al. Serum Neutrophil Gelatinase-Associated Lipocalin Levels and Aortic Stiffness in Noncritical Coronary Artery Disease. *Cardiorenal Med*. 2014;4(3-4):147-154. doi:10.1159/000365200

42. Bu D, Hemdahl A-L, Gabrielsen A, et al. Induction of neutrophil gelatinase-associated lipocalin in vascular injury via activation of nuclear factor-kappaB. *Am J Pathol*. 2006;169(6):2245-2253. doi:10.2353/ajpath.2006.050706

43. Folkesson M, Kazi M, Zhu C, et al. Presence of NGAL/MMP-9 complexes in human abdominal aortic aneurysms. *Thromb Haemost*. 2007;98(2):427-433.

44. Tarjus A, Martínez-Martínez E, Amador C, et al. Neutrophil Gelatinase–Associated Lipocalin, a Novel Mineralocorticoid Biotarget, Mediates Vascular Profibrotic Effects of MineralocorticoidsNovelty and Significance. *Hypertension*. 2015;66(1):158-166. doi:10.1161/HYPERTENSIONAHA.115.05431

45. Tarín C, Fernandez-Garcia CE, Burillo E, et al. Lipocalin-2 deficiency or blockade protects against aortic abdominal aneurysm development in mice. *Cardiovasc Res*. 2016;111(3):262-273. doi:10.1093/cvr/cvw112

46. Yang K, Deng H, Man AWC, et al. Measuring non-polyaminated lipocalin-2 for cardiometabolic risk assessment. *Esc Heart Fail*. 2017;4(4):563-575. doi:10.1002/ehf2.12183

47. Harrison DG, Guzik TJ, Lob HE, et al. Inflammation, Immunity, and Hypertension. *Hypertension*. 2011;57(2):132-140. doi:10.1161/HYPERTENSIONAHA.110.163576

48. Schiffrin EL. The Immune System: Role in Hypertension. *Can J Cardiol*. 2013;29(5):543-548. doi:10.1016/j.cjca.2012.06.009

49. Mortensen RM. Immune Cell Modulation of Cardiac Remodeling. *Circulation*. 2012;125(13):1597-1600. doi:10.1161/CIRCULATIONAHA.112.097832

50. Rickard AJ, Morgan J, Tesch G, Funder JW, Fuller PJ, Young MJ. Deletion of Mineralocorticoid Receptors From Macrophages Protects Against Deoxycorticosterone/Salt-Induced Cardiac Fibrosis and Increased Blood Pressure. *Hypertension*. 2009;54(3):537-543. doi:10.1161/HYPERTENSIONAHA.109.131110

51. Bene NC, Alcaide P, Wortis HH, Jaffe IZ. Mineralocorticoid receptors in immune cells: Emerging role in cardiovascular disease. *Steroids*. 2014;91:38-45.

doi:10.1016/j.steroids.2014.04.005
52. Sun XN, Li C, Liu Y, et al. T Cell Mineralocorticoid Receptor Controls Blood Pressure by Regulating Interferon Gamma. *Circ Res*. Published online March 15, 2017:CIRCRESAHA.116.310480. doi:10.1161/CIRCRESAHA.116.310480
53. Amador CA, Barrientos V, Peña J, et al. Spironolactone decreases DOCA-salt-induced organ damage by blocking the activation of T helper 17 and the downregulation of regulatory T lymphocytes. *Hypertens Dallas Tex 1979*. 2014;63(4):797-803. doi:10.1161/HYPERTENSIONAHA.113.02883
54. Aigner F, Maier HT, Schwelberger HG, et al. Lipocalin-2 Regulates the Inflammatory Response During Ischemia and Reperfusion of the Transplanted Heart. *Am J Transplant*. 2007;7(4):779-788. doi:10.1111/j.1600-6143.2006.01723.x
55. Sickinger S, Maier H, König S, et al. Lipocalin-2 as mediator of chemokine expression and granulocyte infiltration during ischemia and reperfusion. *Transpl Int*. 2013;26(7):761-769. doi:10.1111/tri.12116
56. Schroll A, Eller K, Feistritzer C, et al. Lipocalin-2 ameliorates granulocyte functionality: Innate immunity. *Eur J Immunol*. 2012;42(12):3346-3357. doi:10.1002/eji.201142351
57. Nguyen VT, Farman N, Palacios-Ramirez R, et al. Cutaneous Wound Healing in Diabetic Mice Is Improved by Topical Mineralocorticoid Receptor Blockade. *J Invest Dermatol*. 2020;140(1):223-234.e7. doi:10.1016/j.jid.2019.04.030
58. Ye D, Yang K, Zang S, et al. Lipocalin-2 mediates non-alcoholic steatohepatitis by promoting neutrophil-macrophage crosstalk via the induction of CXCR2. *J Hepatol*. 2016;65(5):988-997. doi:10.1016/j.jhep.2016.05.041
59. Young MJ, Rickard AJ. Mechanisms of mineralocorticoid salt-induced hypertension and cardiac fibrosis. *Mol Cell Endocrinol*. 2012;350(2):248-255. doi:10.1016/j.mce.2011.09.008
60. Yu C, Gong R, Rifai A, Tolbert EM, Dworkin LD. Long-term, high-dosage candesartan suppresses inflammation and injury in chronic kidney disease: nonhemodynamic renal protection. *J Am Soc Nephrol JASN*. 2007;18(3):750-759. doi:10.1681/ASN.2006070770
61. Wolf G, Ziyadeh FN, Thaiss F, et al. Angiotensin II stimulates expression of the chemokine RANTES in rat glomerular endothelial cells. Role of the angiotensin type 2 receptor. *J Clin Invest*. 1997;100(5):1047-1058.
62. Krensky AM, Ahn Y-T. Mechanisms of disease: regulation of RANTES (CCL5) in

renal disease. *Nat Clin Pract Nephrol*. 2007;3(3):164-170. doi:10.1038/ncpneph0418

63. Krebs C, Fraune C, Schmidt-Haupt R, et al. CCR5 deficiency does not reduce hypertensive end-organ damage in mice. *Am J Hypertens*. 2012;25(4):479-486. doi:10.1038/ajh.2011.243

64. Shappell SB, Gurpinar T, Lechago J, Suki WN, Truong LD. Chronic obstructive uropathy in severe combined immunodeficient (SCID) mice: lymphocyte infiltration is not required for progressive tubulointerstitial injury. *J Am Soc Nephrol JASN*. 1998;9(6):1008-1017. doi: 10.1681/ASN.V961008

65. Tapmeier TT, Fearn A, Brown K, et al. Pivotal role of CD4+ T cells in renal fibrosis following ureteric obstruction. *Kidney Int*. 2010;78(4):351-362. doi:10.1038/ki.2010.177

66. Liu L, Kou P, Zeng Q, et al. CD4+ T Lymphocytes, Especially Th2 Cells, Contribute to the Progress of Renal Fibrosis. *Am J Nephrol*. 2012;36(4):386-396. doi:10.1159/000343283

67. Ho I-C, Miaw S-C. Regulation of IL-4 Expression in Immunity and Diseases. *Adv Exp Med Biol*. 2016;941:31-77. doi:10.1007/978-94-024-0921-5_3

68. Liang H, Zhang Z, Yan J, et al. The IL-4 receptor α has a critical role in bone marrow-derived fibroblast activation and renal fibrosis. *Kidney Int*. 2017;92(6):1433-1443. doi:10.1016/j.kint.2017.04.021

69. Yan J, Zhang Z, Yang J, Mitch WE, Wang Y. JAK3/STAT6 Stimulates Bone Marrow–Derived Fibroblast Activation in Renal Fibrosis. *J Am Soc Nephrol*. 2015;26(12):3060-3071. doi:10.1681/ASN.2014070717

70. Weng S-Y, Wang X, Vijayan S, et al. IL-4 Receptor Alpha Signaling through Macrophages Differentially Regulates Liver Fibrosis Progression and Reversal. *EBioMedicine*. 2018;29:92-103. doi:10.1016/j.ebiom.2018.01.028

71. Ong C, Wong C, Roberts CR, Teh HS, Jirik FR. Anti-IL-4 treatment prevents dermal collagen deposition in the tight-skin mouse model of scleroderma. *Eur J Immunol*. 1998;28(9):2619-2629. doi:10.1002/(SICI)1521-4141(199809)28:09<2619::AID-IMMU2619>3.0.CO;2-M

72. Peng H, Sarwar Z, Yang X-P, et al. Profibrotic Role for Interleukin-4 in Cardiac Remodeling and Dysfunction. *Hypertension*. 2015;66(3):582-589. doi:10.1161/HYPERTENSIONAHA.115.05627

73. Kanellakis P, Ditiatkovski M, Kostolias G, Bobik A. A pro-fibrotic role for interleukin-4 in cardiac pressure overload. *Cardiovasc Res*. 2012;95(1):77-85. doi:10.1093/cvr/cvs142

74. Roselló-Lletí E, Rivera M, Bertomeu V, Cortés R, Jordán A, González-Molina A. [Interleukin-4 and cardiac fibrosis in patients with heart failure]. *Rev Esp Cardiol*. 2007;60(7):777-780.
75. Bonnard B, Martínez-Martínez E, Fernández-Celis A, et al. Antifibrotic effect of novel neutrophil gelatinase-associated lipocalin inhibitors in cardiac and renal disease models. *Sci Rep*. 2021;11(1):2591. doi:10.1038/s41598-021-82279-0

Figure 1. NGAL inactivation in macrophages (MΦ KO NGAL) blunts mineralocorticoid-induced kidney fibrosis. NAS-induced renal fibrosis stained by Sirius Red **(A)** and mRNA overexpression of pro-fibrotic markers, such as collagen I, fibronectin and αSMA **(B)** in MΦ WT mice (MΦ WT NAS) were prevented in MΦ KO NGAL NAS mice**. (C)** mRNA overexpression of proinflammatory markers (IL1β, IL6, TNFα, MCP1 and CCL5) induced by NAS challenge, was blunted for TNFα, MCP1 and CCL5 in whole kidney from MΦ KO NGAL NAS mice. **(D)** NAS induced mature macrophages $CD11b^{+}$ $F4/80^{high}$ infiltration in kidney from MΦ WT and MΦ KO mice. One-way ANOVA was used for statistical analysis, $n = 5\text{-}8$. $^{*}P < 0.05$. Absolute count of challenged by NAS (6w). **(E)** Lower expression of proinflammatory markers (IL1β, TNFα, MCP1 and CCL5) in sorted $CD11b^{+}$ $F4/80^{high}$ kidney cells from MΦ KO NGAL mice compared to MΦ WT challenged by NAS 8 days (8d). Student t-tests were used for statistical analysis, $n = 4\text{-}5$. $^{*}P < 0.05$. Scale bare 10 μm.

Figure 2. NGAL is required for proinflammatory cytokine/chemokine expression in cultured peritoneal macrophages upon ex vivo aldosterone-salt stimulation. **(A)** Heat map representing normalized gene expression with significant differences between cultured peritoneal macrophages from WT (MΦ WT) and KO NGAL (MΦ KO NGAL) mice co-treated with aldosterone and salt (A/S). Gene expression is defined by the color gradient, with low expression shown in blue to high expression in red. False discovery changes two-stage step-up method for Benjamini, Krieger and Yekutieli was performed for statistical analysis. $n = 5$. $q < 0.05$. **(B)** Co-treatment A/S increased gene expression of various proinflammatory markers in MΦ WT + A/S blunted in MΦ KO NGAL + A/S for IL6 and CCL5. Two-way ANOVA was used for statistical analysis, $n = 5$. $^{*}P < 0.05$.

Figure 3. Pharmacological CCL5 receptor antagonism (MARA) blunts NAS-induced renal fibrosis. NAS-induced renal fibrosis stained by Sirius Red **(A)** and protein level of pro-fibrotic markers, such as collagen I, fibronectin and αSMA **(B)** in WT mice (NAS) were limited in NAS + MARA NAS mice**. (C)** mRNA overexpression of proinflammatory markers (IL1β, IL6, TNFα, MCP1 and CCL5) is similar in both groups exposed to NAS challenge. One-way ANOVA was used for statistical analysis, n = 7-10. *$P < 0.05$. Scale bare 10 μm.

Figure 4. CCL5 and NGAL are involved in T helper lymphocytes (Th) recruitment induced by NAS challenge. **(A)** NAS challenge induced Th cells ($CD3^+$ $CD4^+$) in kidney associated with an increase of IL4 expression expressed by Th cells **(B)**. Student t-tests were used for statistical analysis. Student t-tests were used for statistical analysis, n = 5-7. *$P < 0.05$. In whole kidney, NAS challenge increased IL4 mRNA expression blunted in mice treated with CCL5 receptor antagonism (NAS + MARA) **(C)** and prevented by NGAL deletion in macrophages (MΦ KO NGAL NAS) **(D)**. One-way ANOVA was used for statistical analysis, n = 5-10. *$P < 0.05$.

Figure 5. The Th2-cytokine IL4 is involved in the profibrotic effect induced by NAS in kidney mice. IL4 induced STAT6 phosphorylation **(A)** associated with an increase of profibrotic markers **(B)** in mouse kidney fibroblasts prevented by an inhibitor of STAT6 (STAT6i). One-way ANOVA was used for statistical analysis, n = 4-12. *$P < 0.05$. **(C)** Renal fibrosis stained by Sirius Red **(C)** and protein level of pro-fibrotic markers, such as collagen I and fibronectin were increased **(D)** in NAS treated mice injected with IgG1 isotype control antibody (NAS (6w) + IgG1) prevented by anti-IL4 neutralizing antibody injection (NAS (6w) + IL4 AB). One-way ANOVA was used for statistical analysis, n = 6-7. *$P < 0.05$. Scale bare 10 μm.

General characteristics	MΦ CTL CONTROL	MΦ CTL NAS	MΦ KO NGAL NAS
Body weight (g)	29.00±0.41	24.13±0.55*	24.22±0.55*
Kidney weight/Tibia Length (mg/mm)	9.06±0.36	17.66±0.61*	18.61±0.91*
Systolic Blood Pressure (mmHg)	109.8±1.50	136.7±3.68*	120.9±2.75*†
Plasma Creatinine level (μM)	9.89±0.22	13.54±0.84*	14.91±1.13*

General characteristics	CONTROL	NAS	NAS + MARA
Body weight (g)	28.12±0.66	26.03±0.27*	25.67±0.37*
Kidney weight/Tibia Length (mg/mm)	9.03±0.28	15.81±0.60*	15.79±0.50*
Systolic Blood Pressure (mmHg)	118.6±1.90	130.3±1.38*	131.3±2.20*
Plasma Creatinine level (μM)	11.02±0.54	18.60±0.67*	16.41±1.13*

General characteristics	CONTROL	NAS + IgG1	NAS + IL4 AB
Body weight (g)	26.20±0.26	24.56±0.38	24.93±0.50
Kidney weight/Tibia Length (mg/mm)	8.64±0.21	19.30±0.73*	17.57±0.43*
Systolic Blood Pressure (mmHg)	121.2±4.11	141.7±2.70*	142.2±3.07*
Plasma Creatinine level (μM)	8.48±0.63	12.40±0.84*	12.22±0.41*

Table 1. Physiological parameters in NAS models.
One-way ANOVA was used for statistical analysis. n=5-10, *p<0.05 *vs* MΦ CONTROL or CONTROL, †p<0.05 *vs* MΦ NAS

Figure 1

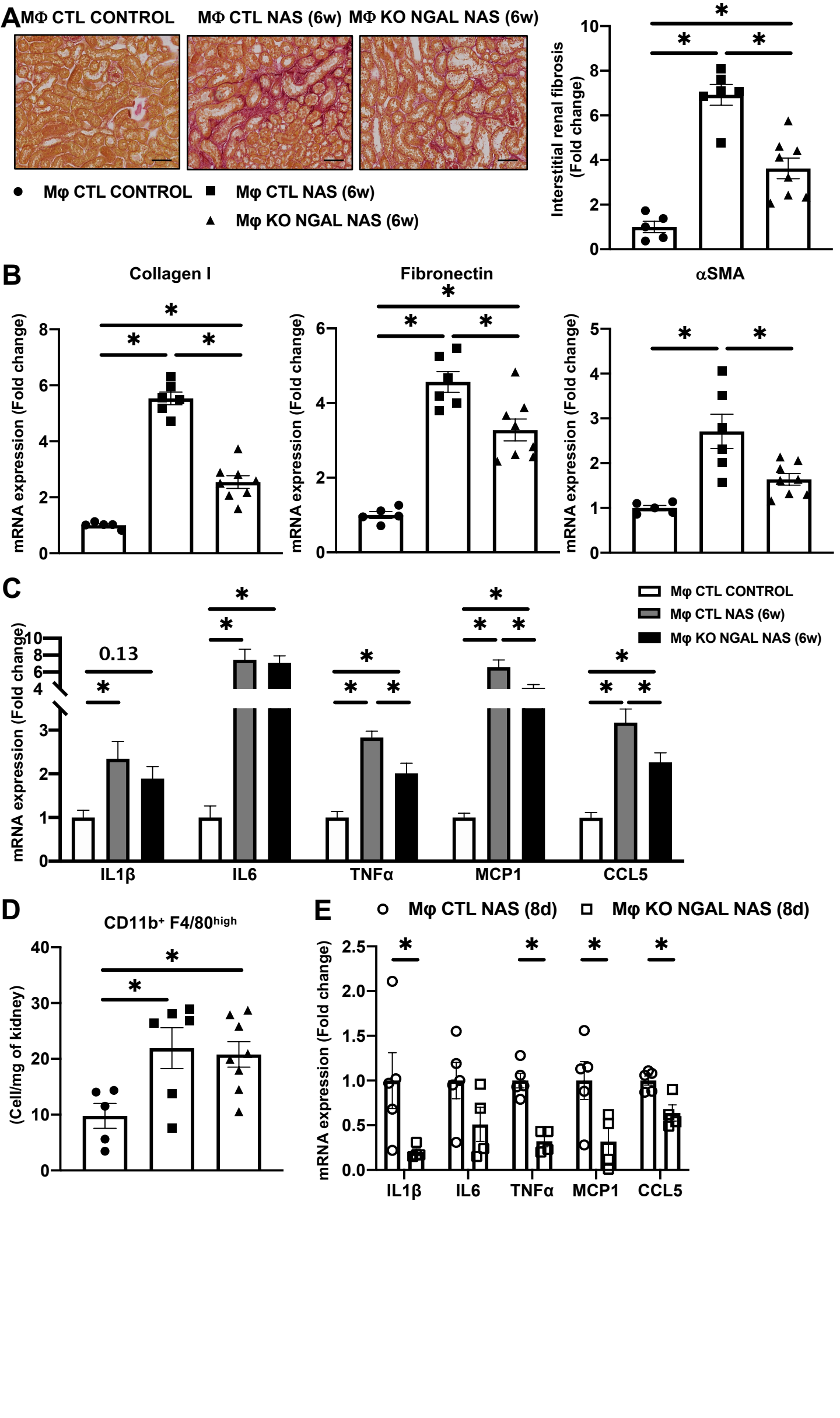
A
MΦ CTL CONTROL
MΦ CTL NAS (6w)
MΦ KO NGAL NAS (6w)
Mφ CTL CONTROL
Mφ CTL NAS (6w)
Mφ KO NGAL NAS (6w)
Interstitial renal fibrosis (Fold change)
B
Collagen I
Fibronectin
αSMA
mRNA expression (Fold change)
C
Mφ CTL CONTROL
Mφ CTL NAS (6w)
Mφ KO NGAL NAS (6w)
mRNA expression (Fold change)
0.13
IL1β
IL6
TNFα
MCP1
CCL5
D
CD11b+ F4/80high
(Cell/mg of kidney)
E
Mφ CTL NAS (8d)
Mφ KO NGAL NAS (8d)
mRNA expression (Fold change)
IL1β
IL6
TNFα
MCP1
CCL5

Figure 2

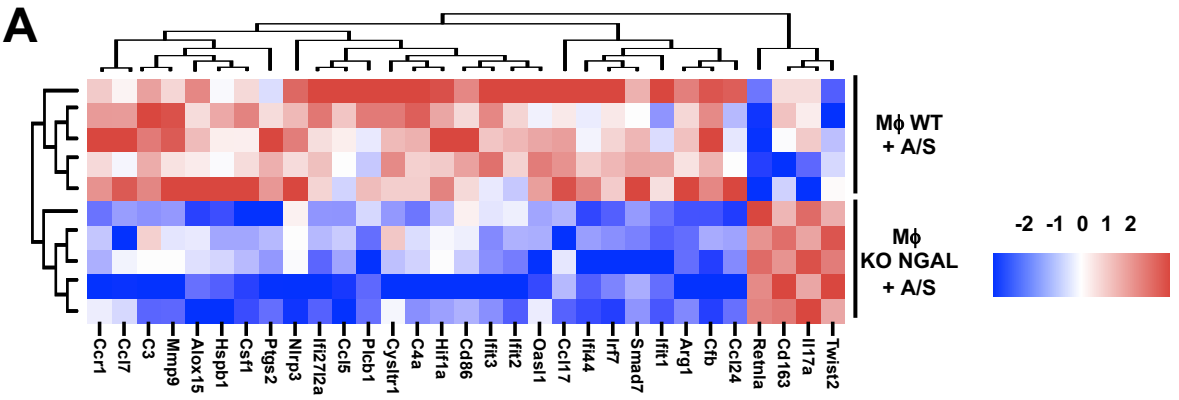
A
Mϕ WT
+ A/S
Mϕ
KO NGAL
+ A/S
-2 -1 0 1 2
Ccr1
Ccl7
C3
Mmp9
Alox15
Hspb1
Csf1
Ptgs2
Nlrp3
Ifi27l2a
Ccl5
Plcb1
Cysltr1
C4a
Hif1a
Cd86
Ifit3
Ifit2
Oasl1
Ccl17
Ifi44
Irf7
Smad7
Ifit1
Arg1
Cfb
Ccl24
Retnla
Cd163
Il17a
Twist2

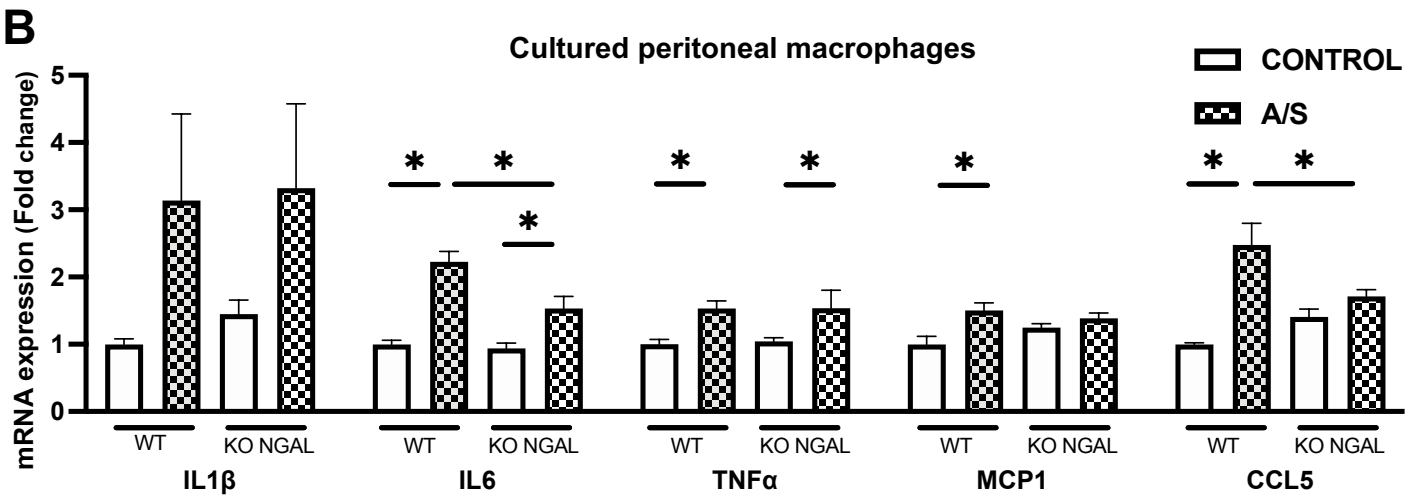
B
Cultured peritoneal macrophages
CONTROL
A/S
mRNA expression (Fold change)
0
1
2
3
4
5
WT
KO NGAL
IL1β
IL6
TNFα
MCP1
CCL5

Figure 3

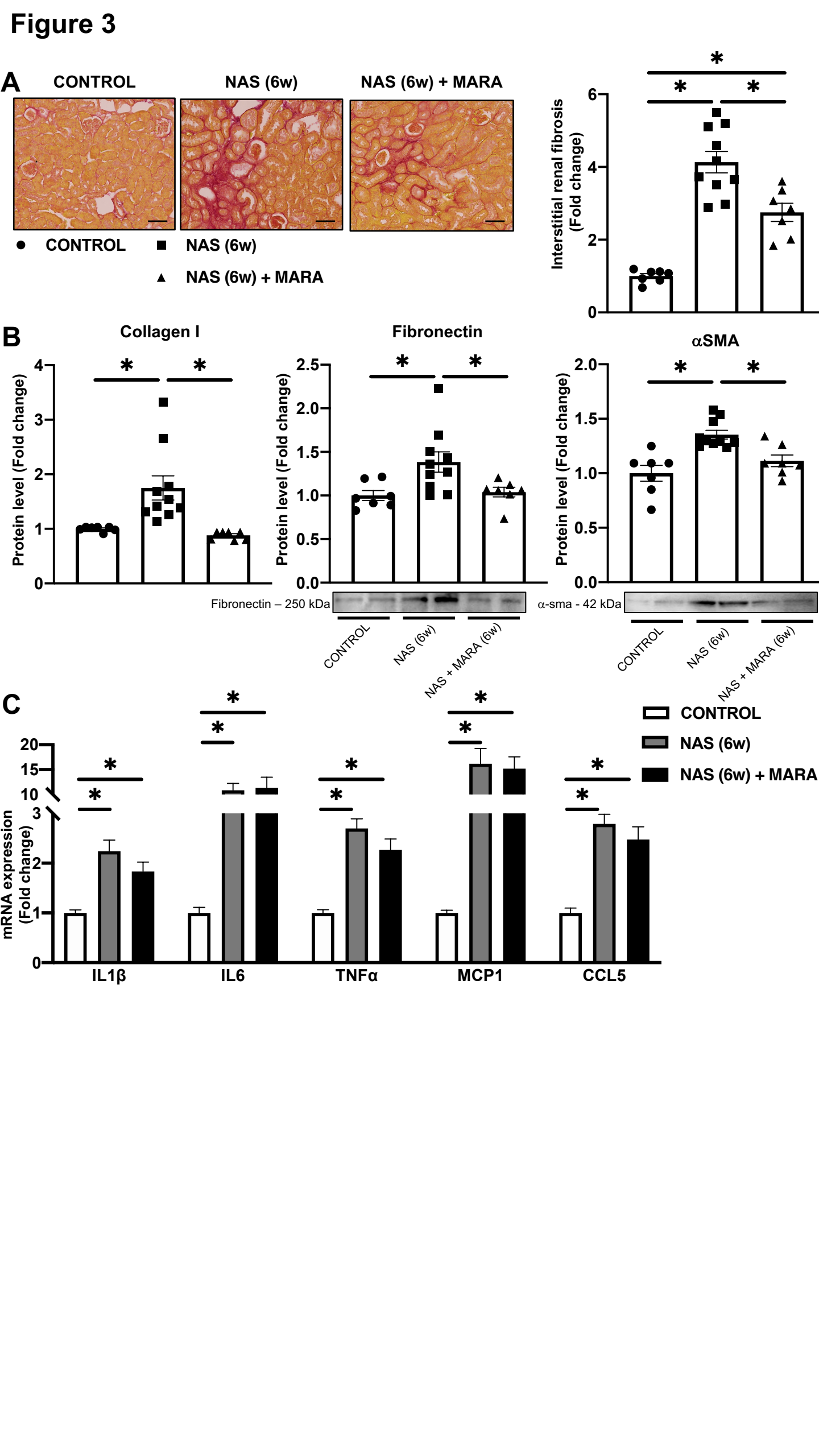
A
CONTROL
NAS (6w)
NAS (6w) + MARA
CONTROL
NAS (6w)
NAS (6w) + MARA
Interstitial renal fibrosis (Fold change)
B
Collagen I
Fibronectin
αSMA
Protein level (Fold change)
Fibronectin – 250 kDa
α-sma - 42 kDa
CONTROL
NAS (6w)
NAS + MARA (6w)
C
mRNA expression (Fold change)
IL1β
IL6
TNFα
MCP1
CCL5
CONTROL
NAS (6w)
NAS (6w) + MARA

Figure 4

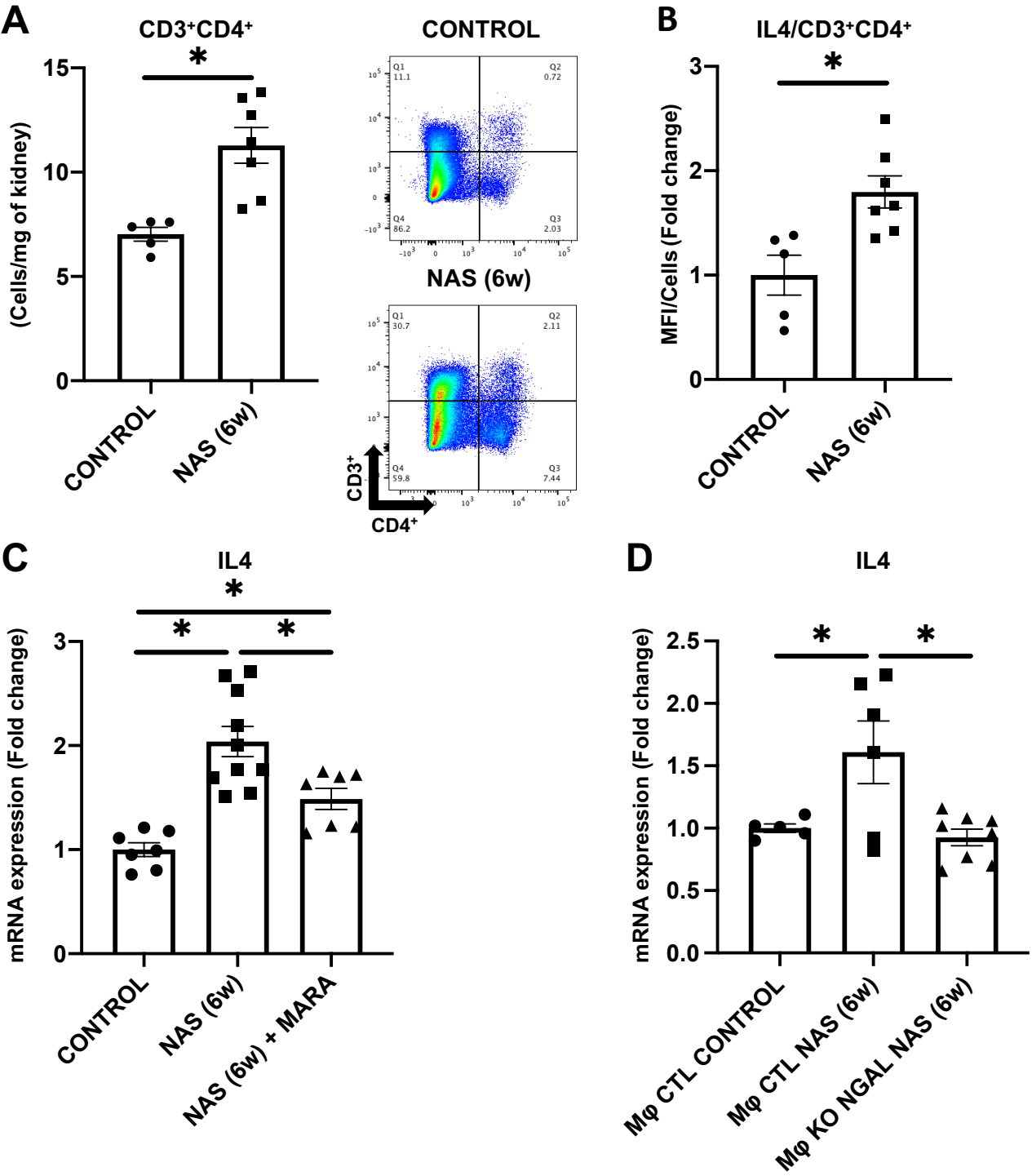
A
CD3⁺CD4⁺
(Cells/mg of kidney)
15
10
5
0
*
CONTROL
NAS (6w)
CONTROL
Q1 11.1
Q2 0.72
Q4 86.2
Q3 2.03
NAS (6w)
Q1 30.7
Q2 2.11
Q4 59.8
Q3 7.44
CD3⁺
CD4⁺
B
IL4/CD3⁺CD4⁺
MFI/Cells (Fold change)
3
2
1
0
*
CONTROL
NAS (6w)
C
IL4
mRNA expression (Fold change)
3
2
1
0
*
*
*
CONTROL
NAS (6w)
NAS (6w) + MARA
D
IL4
mRNA expression (Fold change)
2.5
2.0
1.5
1.0
0.5
0.0
*
*
Mφ CTL CONTROL
Mφ CTL NAS (6w)
Mφ KO NGAL NAS (6w)

Figure 5

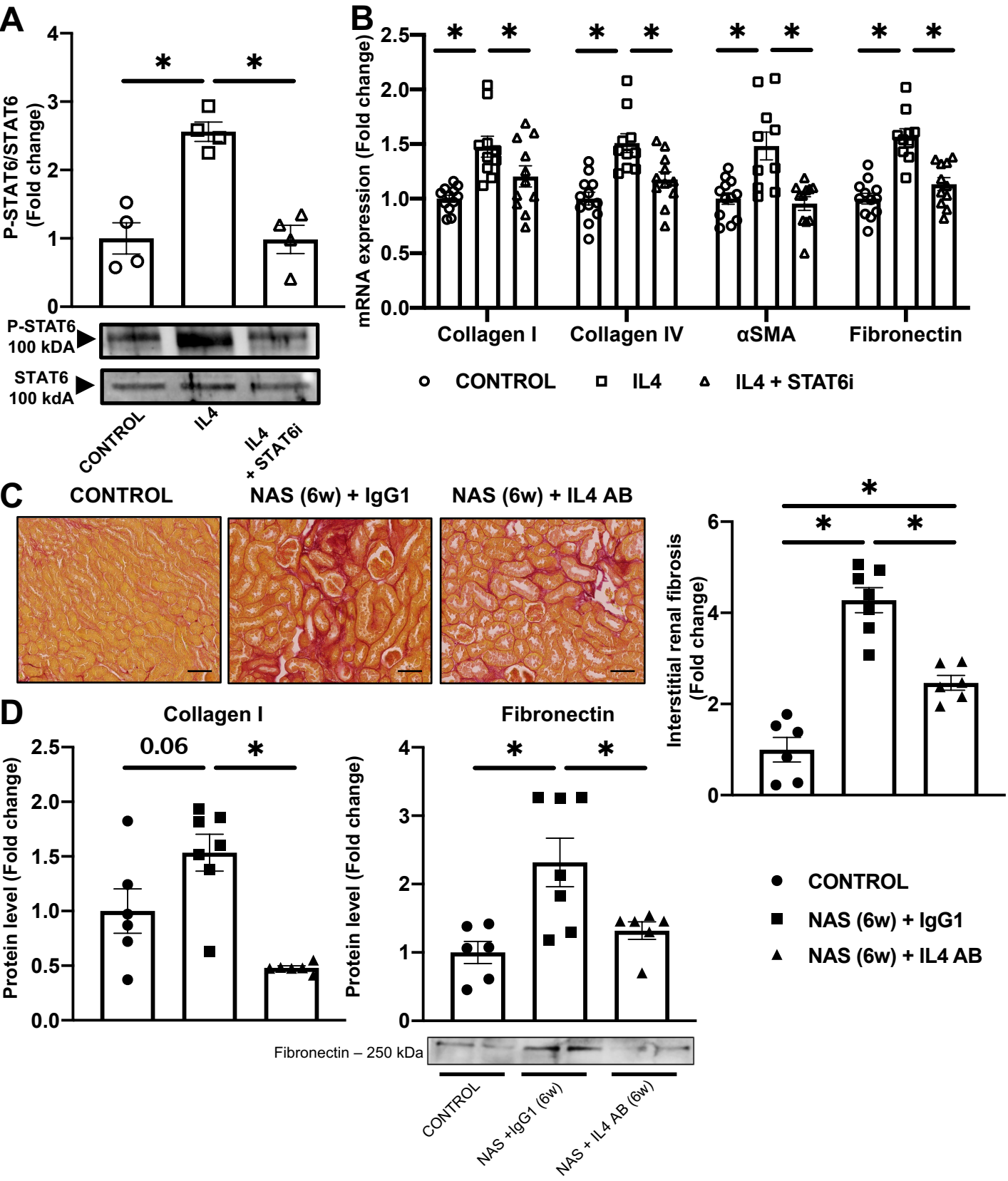
A
P-STAT6/STAT6 (Fold change)
P-STAT6 100 kDA
STAT6 100 kdA
CONTROL
IL4
IL4 + STAT6i
B
mRNA expression (Fold change)
Collagen I
Collagen IV
αSMA
Fibronectin
CONTROL
IL4
IL4 + STAT6i
C
CONTROL
NAS (6w) + IgG1
NAS (6w) + IL4 AB
Interstitial renal fibrosis (Fold change)
CONTROL
NAS (6w) + IgG1
NAS (6w) + IL4 AB
D
Collagen I
0.06
Protein level (Fold change)
Fibronectin
Protein level (Fold change)
Fibronectin – 250 kDa
CONTROL
NAS +IgG1 (6w)
NAS + IL4 AB (6w)

Supplemental Methods

Mice

To assess the global inactivation of Lcn2, we used mice with a total deletion of Lcn2 (KO NGAL)[1] and their WT littermates as control mice (WT). Animals with bone marrow (BM) specific inactivation of NGAL (KO BM) were generated as previously described[2] by irradiating (two irradiations of 5 Greys at 5-hours intervals with a Faxitron irradiator) three-month-old male C57BL/6 wild type mice (WT) (JANVIER LABS, Le Genest-Saint-Isle, France) and then injecting them with 10 million BM cells in the penile vein. Three-month-old male mice with constitutively inactivated NGAL (Knock Out, KO) (for KO BM animals)[3] and WT littermates (for WT BM animals) were used as bone marrow donors (Figure S2A). Two months after the transplantation, mice had NAS challenge for 6 weeks.

Cultured mouse peritoneal macrophages

Peritoneal macrophages (MΦ) were isolated as described previously[4]. Briefly, eight-week-old WT and KO NGAL mice were injected intraperitoneally with 1 ml 3% brewer thioglycolate medium (Sigma-Aldrich). Four days later, mice were sacrificed by cervical dislocation and the peritoneal MΦ collected in cold DPBS. After centrifugation, the pellet containing MΦ was resuspended in culture medium (RPMI medium 1640 + 10% fetal bovine serum (FBS) + 1% penicillin-streptomycin (P/S); ThermoFisher). A total of 1 x 10^6 cells/well were seeded in 12-well plates (Falcon). After 2 h, non-adherent cells were removed by washing with DPBS. The days after, MΦ were then co-treated with aldosterone (10^{-8}M) and NaCl (40 mM) (A/S) for 24 h in culture medium containing charcoal stripped FBS. A portion of MΦ were treated with mannitol (80 mM), as previously described[5], to control for the potential effects of hyperosmolarity. Cultured MΦ were maintained at 37°C in a 5% CO2 humidified incubator.

Mouse kidney fibroblasts

Mouse kidney fibroblasts (MKFs) were isolated from WT mice. Briefly, eight-week-old mice were sacrificed by cervical dislocation and the kidneys removed and rinsed in cold DPBS. The renal cortex was minced and incubated in Dulbecco's modified eagle medium/Nutrient mixture F-12 (DMEM/F12, Sigma-Aldrich) containing 1 mg/ml collagenase A (Roche) for 25 min at 37°C. The digestion was inactivated by adding culture medium (DMEM/F12 + 10% FBS + 1% P/S) and the cell suspension then passed through a 100-µm cell strainer. After centrifugation, the pellet (containing MKFs) was diluted with culture medium and plated in 75-cm^2 culture flasks. After 24 h, MKFs were washed with DPBS before replacement with fresh culture

medium. Thereafter, culture medium was changed every 48 h. Once they were 70 to 80% confluent, MKFs were trypsinized and plated in 12- or 6-well plates. For experiments, MKFs were starved in culture medium containing only 3% FBS. The starved cells were treated with recombinant mouse IL4 protein (100 ng/ml, R&D system) for 6 h for RNA isolation and 24 h for protein analyses. MKFs were maintained at 37°C in a 5% CO2 humidified incubator.

Blood pressure measurements

Systolic blood pressure (SBP) was measured by tail-cuff plethysmography for three consecutive days after two days of training in the same room at the same hour on conscious mice one week before their sacrifice using a BP2000 Visitech device.

Tissue and blood sampling

Kidneys were harvested at sacrifice and rinsed in ice-cold Dulbecco's phosphate buffered saline (DPBS; ThermoFisher). Kidneys were weighed and cut transversally into two parts, one for mRNA and protein extraction and the other for histology. All non-fixed samples were snap frozen in liquid nitrogen and stored at −80 °C.

At sacrifice, blood was collected in heparinized microvette tubes and plasma isolated by centrifugation (1000 x g, 10 min) and stored at −80°C. Plasma creatinine levels were analyzed using a Konelab 20i (ThermoFisher) chemistry analyzer.

Histology

Kidneys were fixed in 4% paraformaldehyde, embedded in paraffin, and 6-µm sections prepared. Sirius red staining was performed to assess renal fibrosis. Images were captured using an Axio Scan Z1 (Zeiss) slide scanner. Renal fibrosis was analyzed using the bioimage analysis software QuPath[6].

Gene expression profiling

RNA (200 ng) was hybridized with probes from the Nanostring Inflammation panel that includes 254 genes involved in several inflammatory pathways, following the provider's instructions (sequences and gene list available at https://www.nanostring.com/products/gene-expression-panels/gene-expression-panels-overview/ncounter-inflammation-panels). Gene expression was analyzed using NanoString nSolver Analysis V4.0 software.

qPCR

Kidneys were homogenized in TRIzol (Life Technologies) using FastPrep beads (MP-Bio). RNA from cells (MΦ and MKFs) was obtained by simply adding TRIzol to the wells. RNA was obtained from sorted cells using RNeasy Mini Kits (Qiagen). cDNAs were generated using

the M-MLV reverse transcriptase kit (Invitrogen) or Superscript II (Invitrogen) for RNA extracted from sorted cells and qPCR was performed as previously described. Briefly, transcript levels were analyzed using a CFX396 apparatus (BioRad). The reactions were performed in duplicate for each sample using the IQ SYBR Green supermix Kit (BioRad). Gene expression was normalized using the geometric mean of multiple internal reference genes (UBC, HPRT), as previously described[7]. Values under the control conditions were set to 1 for each gene. The sequences of the specific primers were: *UBC*, sense: 5'-CGGAGTCGCCCGAGGTCACA-3', anti-sense: 5'-GGGCTCGACCTCCAGGGTGAT-3'; *HPRT*, sense: 5'-TCTAACTTTAACTGGAAAGAATGTC-3', anti-sense: 5'-TCCTTTTCACCAGCAAGCT-3'; *collagen I*, sense: 5'-CCCCGGGACTCCTGGACTT-3', anti-sense: 5'-GCTCCGACACGCCCTCTCTC-3'; *collagen IV*, sense: 5'-ATTCCTCGTGATGCACACC-3', anti-sense: 5'-GTGGGCTTCTTGACATCTC-3'; *fibronectin*, sense: 5'-CCTACGGCCACTGTGTCACC-3', anti-sense: 5'-AGTCTGGGTCACGGCTGTCT-3'; *IL1β*, sense: 5'-TCGCTCAGGGTCACAAGAAAC-3', anti-sense: 5'-CATCAGAGGCAAGGAGGAAAAC-3'; *IL6*, sense : 5'-CTCTGGGAAATCGTGGAAATG-3', anti-sense: 5'-AAGTGCATCATCGTTGTTCATACA-3'; *TNFα*, sense: 5'-GCCTCTTCTCATTCCTGCTTG -3', anti-sense 5'-CTGATGAGAGGGAGGCCATT-3'; *MCP1*, sense: 5'-GGCTGGAGAGCTACAAGAGG-3', anti-sense: 5'-TCTTGAGCTTGGTGACAAAAAC-3'; *CCL5*, sense: 5'-GCCCTCACCATCATCCTCACT-3', anti-sense: 5'-GGCGGTTCCTTCGAGTGACA-3'; *CD3*, sense: 5'-CTGCTACACACCAGCCTCAAA-3', anti-sense: 5'-TGGCTACTGCTGTCAGGTCC-3'; *CD8*, sense: 5'-CGGATTGGACTTCGCCTGTG-3', anti-sense: 5'-GGGACATTTGCAAACACGCT-3'; *CD4*, sense: 5'-TTTGCTGGTTCTGGCAACCT-3', anti-sense 5'-ATCTTGGGAGAGGTAGGTCCC-3'; *IFNγ*, sense: 5'-TCAGCAACAGCAAGGCGAAA -3', anti-sense: 5'-CATTGAATGCTTGGCGCTGG -3'; *IL4*, sense: 5'-ACAGGAGGAAGGGACGCCAT-3', anti-sense: 5'-GAAGCCCTACAGACGAGCTCA -3'; *αSMA*, sense: 5'-TGTGCTGGACTCTGGAGATG-3', anti-sense: 5'-GAAGGAATAGCCACGCTCAG-3'.

Western Blotting

Renal proteins were extracted in 1% SDS buffer containing PhosSTOP phosphatase inhibitor (Roche) and complete protease inhibitor (Roche) reagents. The protein concentration was estimated using the Pierce method. Membranes were incubated overnight (4°C) with the respective antibodies: anti-mouse αSMA (Abcam, 1/100), anti-mouse fibronectin (Sigma,

1/100), anti-mouse collagen IV (Abcam, 1/100), anti-mouse STAT6 (Abcam, 1/200), and anti-mouse Phospho-Stat6 (Abcam, 1/500). A chemiluminescent signal was produced using ECL+ solution and detected using a ChemiDoc image analyzer (BioRad). Relative densitometry was performed using Image Lab (BioRad) software. Protein normalization was performed using stain-free imaging technology (BioRad).

ELISA

Collagen I (R&D System, DY6220-05) levels were analyzed in kidney tissue and cell supernatants by ELISA according to the manufacturer's instructions.

Supplemental References

1 Berger T, Togawa A, Duncan GS, Elia AJ, You-Ten A, Wakeham A, Fong HEH, Cheung CC, Mak TW. Lipocalin 2-deficient mice exhibit increased sensitivity to Escherichia coli infection but not to ischemia-reperfusion injury. *Proc Natl Acad Sci U S A* 2006; **103**: 1834–1839. doi:10.1073/pnas.0510847103

2 Buonafine M, Martínez-Martínez E, Amador C, Gravez B, Ibarrola J, Fernández-Celis A, El Moghrabi S, Rossignol P, López-Andrés N, Jaisser F. Neutrophil Gelatinase-Associated Lipocalin from immune cells is mandatory for aldosterone-induced cardiac remodeling and inflammation. *J Mol Cell Cardiol* 2018; **115**: 32–38. doi:10.1016/j.yjmcc.2017.12.011

3 Tarjus A, Martínez-Martínez E, Amador C, Latouche C, El Moghrabi S, Berger T, Mak TW, Fay R, Farman N, Rossignol P, others. Neutrophil Gelatinase–Associated Lipocalin, a Novel Mineralocorticoid Biotarget, Mediates Vascular Profibrotic Effects of Mineralocorticoids. *Hypertension* 2015; **66**: 158–166.

4 Zhang X, Goncalves R, Mosser DM. The isolation and characterization of murine macrophages. *Curr Protoc Immunol* 2008; **Chapter 14**: Unit 14.1. doi:10.1002/0471142735.im1401s83

5 Hucke S, Eschborn M, Liebmann M, Herold M, Freise N, Engbers A, Ehling P, Meuth SG, Roth J, Kuhlmann T, Wiendl H, Klotz L. Sodium chloride promotes pro-inflammatory macrophage polarization thereby aggravating CNS autoimmunity. *J Autoimmun* 2016; **67**: 90–101. doi:10.1016/j.jaut.2015.11.001

6 Bankhead P, Loughrey MB, Fernández JA, Dombrowski Y, McArt DG, Dunne PD, McQuaid S, Gray RT, Murray LJ, Coleman HG, James JA, Salto-Tellez M, Hamilton PW.

QuPath: Open source software for digital pathology image analysis. *Sci Rep* 2017; **7**: 1–7. doi:10.1038/s41598-017-17204-5

7 Vandesompele J, De Preter K, Pattyn F, Poppe B, Van Roy N, De Paepe A, Speleman F. Accurate normalization of real-time quantitative RT-PCR data by geometric averaging of multiple internal control genes. *Genome Biol* 2002; **3**: research0034.1. doi:10.1186/gb-2002-3-7-research0034

Supplemental Figures

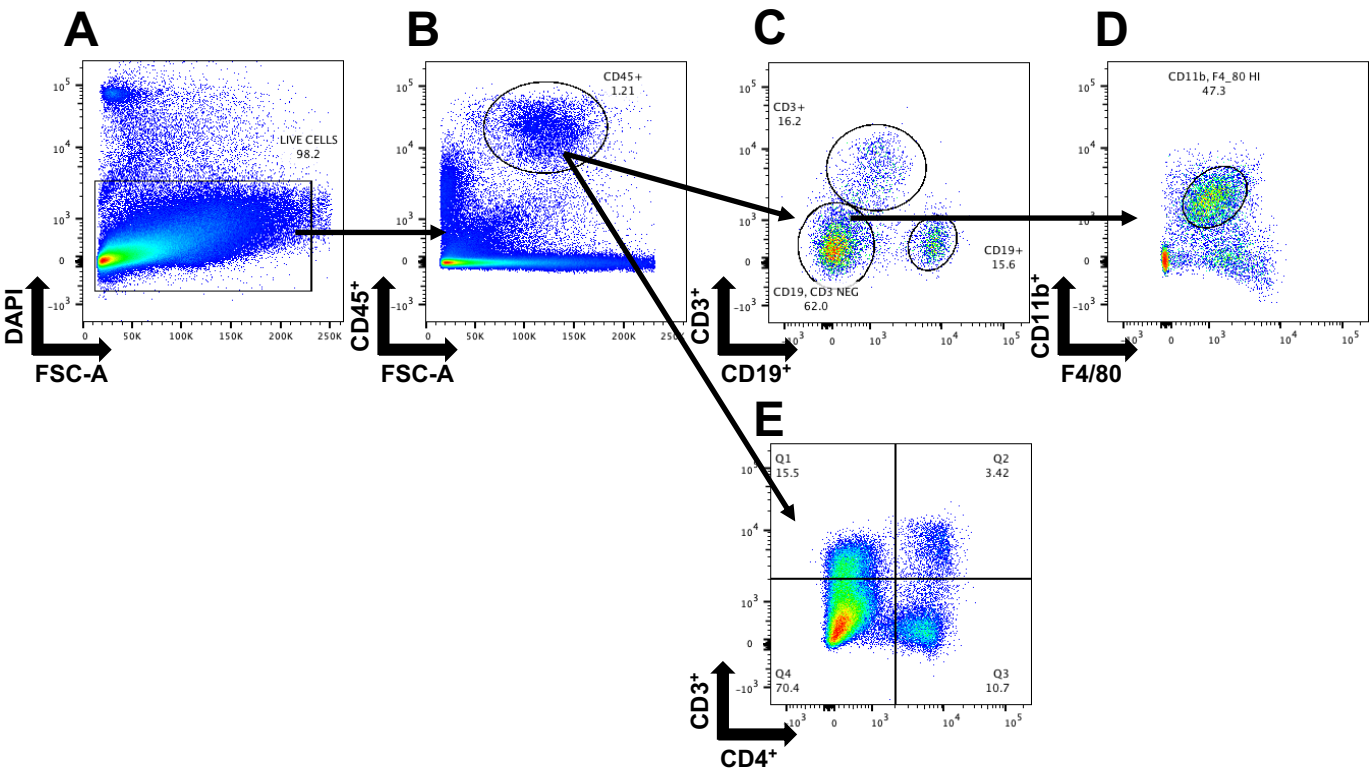

Figure S1. Strategy used for flow cytometry analyses and sorted macrophages. **(A)** Only live cells were explored for flow cytometry analysis. **(B)** Leukocytes were stained by the common antigen CD45. **(C)** Population of T cells ($CD3^+$), B cells ($CD19^+$) were obtained from live cells and $CD45^+$ cells. **(D)** Mature macrophages ($CD11b^+$ $F4/80^{high}$) count and isolated from kidney were gated in $CD3^-$ $CD19^-$. **(E)** $CD3^+$ $CD4^+$ cells count were gated in $CD45^+$.

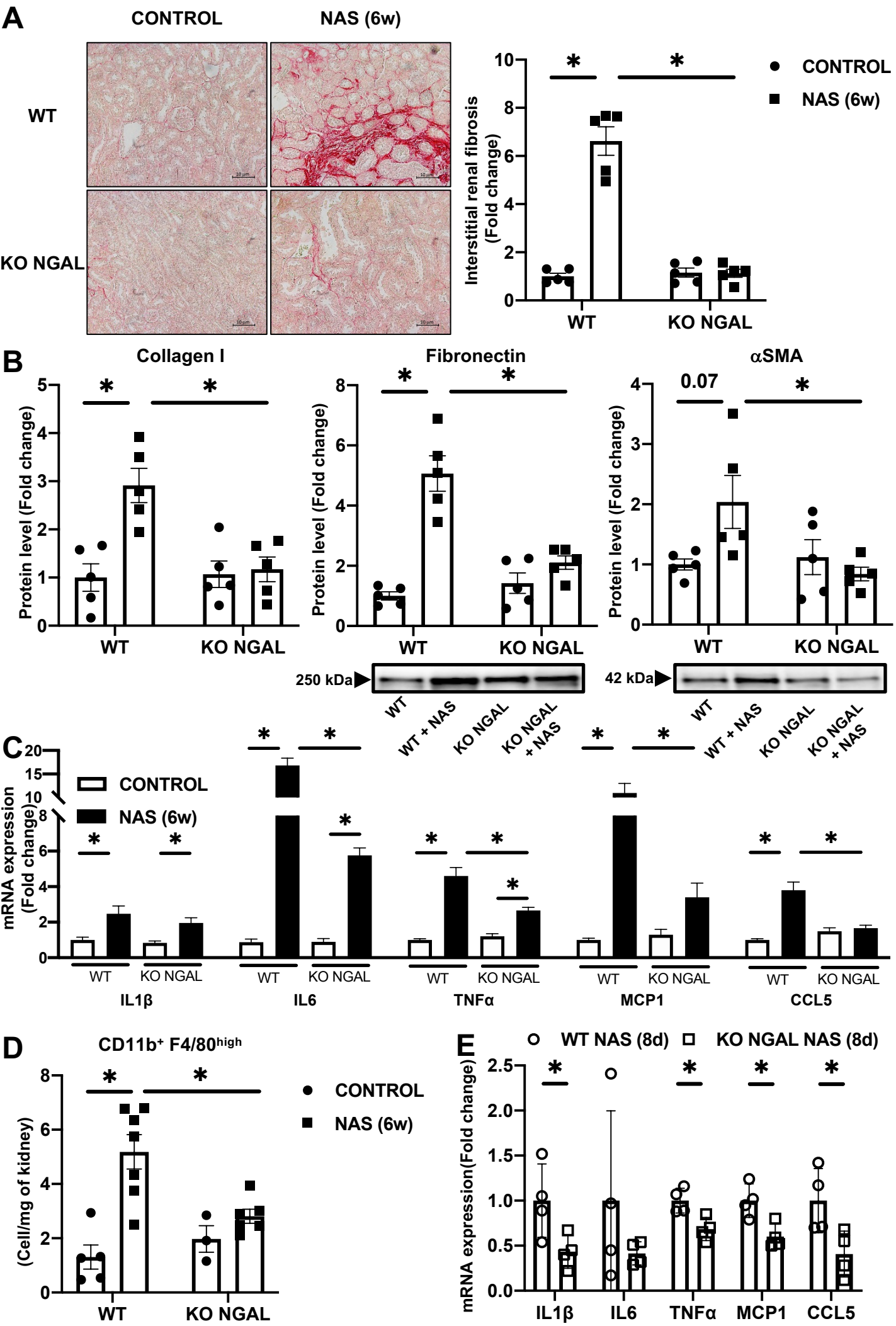

Figure S2. NGAL deletion prevents kidney injury induced by NAS for six weeks. **(A)** Representative images of Sirius Red staining with quantification**. (B)** Protein expression of pro-fibrotic markers, such as collagen I, fibronectin, αSMA. **(C)** Gene expression of proinflammatory markers analyzed in whole kidney from WT and KO NGAL mice exposed to NAS challenge. **(D)** Absolute count of mature macrophages $CD11b^{+}$ $F4/80^{high}$ in kidney from WT and KO NGAL mice challenged by NAS (6w). **(E)** Gene expression in sorted $CD11b^{+}$ $F4/80^{high}$ kidney from WT and KO NGAL mice challenged by NAS (8d). *$P < 0.05$. Two-way ANOVA was used for statistical analysis of 4 groups, n = 3-7. Student t-tests were used for statistical analysis of 2 groups, $n = 4$. *$P< 0.05$. Scale bare 10 μm.

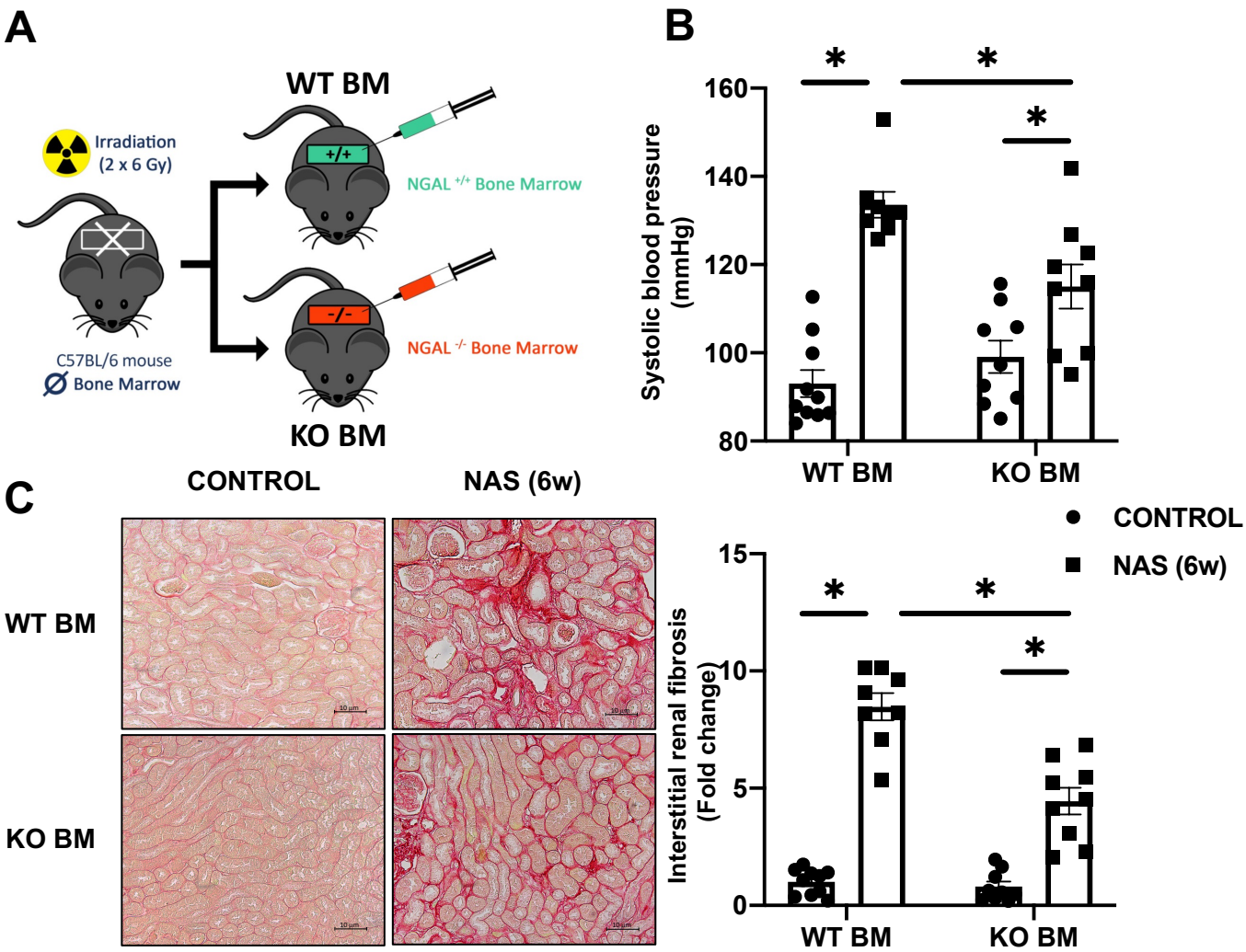

Figure S3. NGAL deletion in myeloid cells prevents renal fibrosis induced by NAS. **(A)** Representative drawing of NGAL depletion in myeloid cells (KO BM) and their controls (WT BM). **(B)** Systolic blood pressure measurements. **(C)** Representative images of Sirius Red staining with quantification. Two-way ANOVA was used for statistical analysis, n = 8-10. *P< 0.05

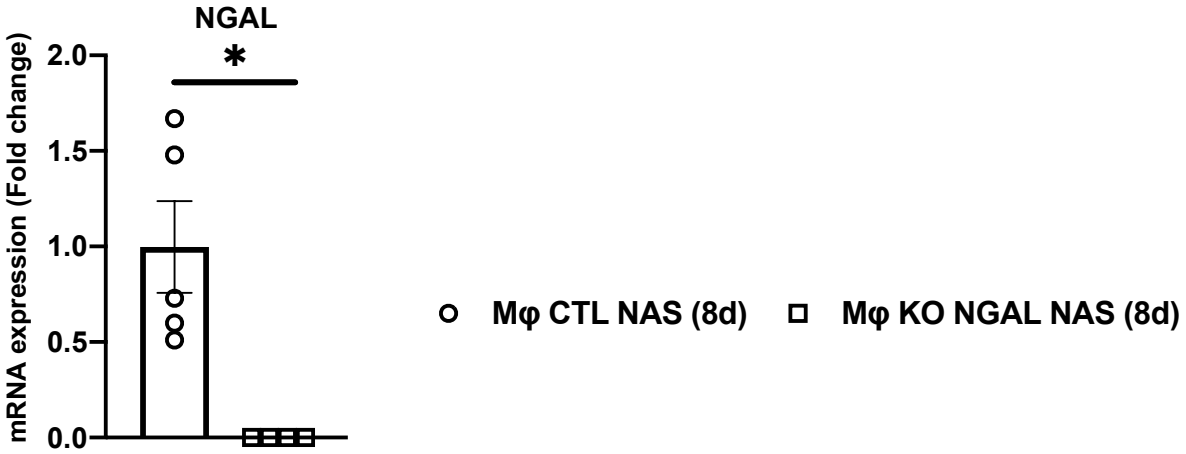

Figure S4. NGAL mRNA expression in sorted renal macrophages from MΦ CTL and MΦ KO NGAL mice challenged by NAS (8d). Student t-test was used for statistical analysis, n = 4-5. *P< 0.05

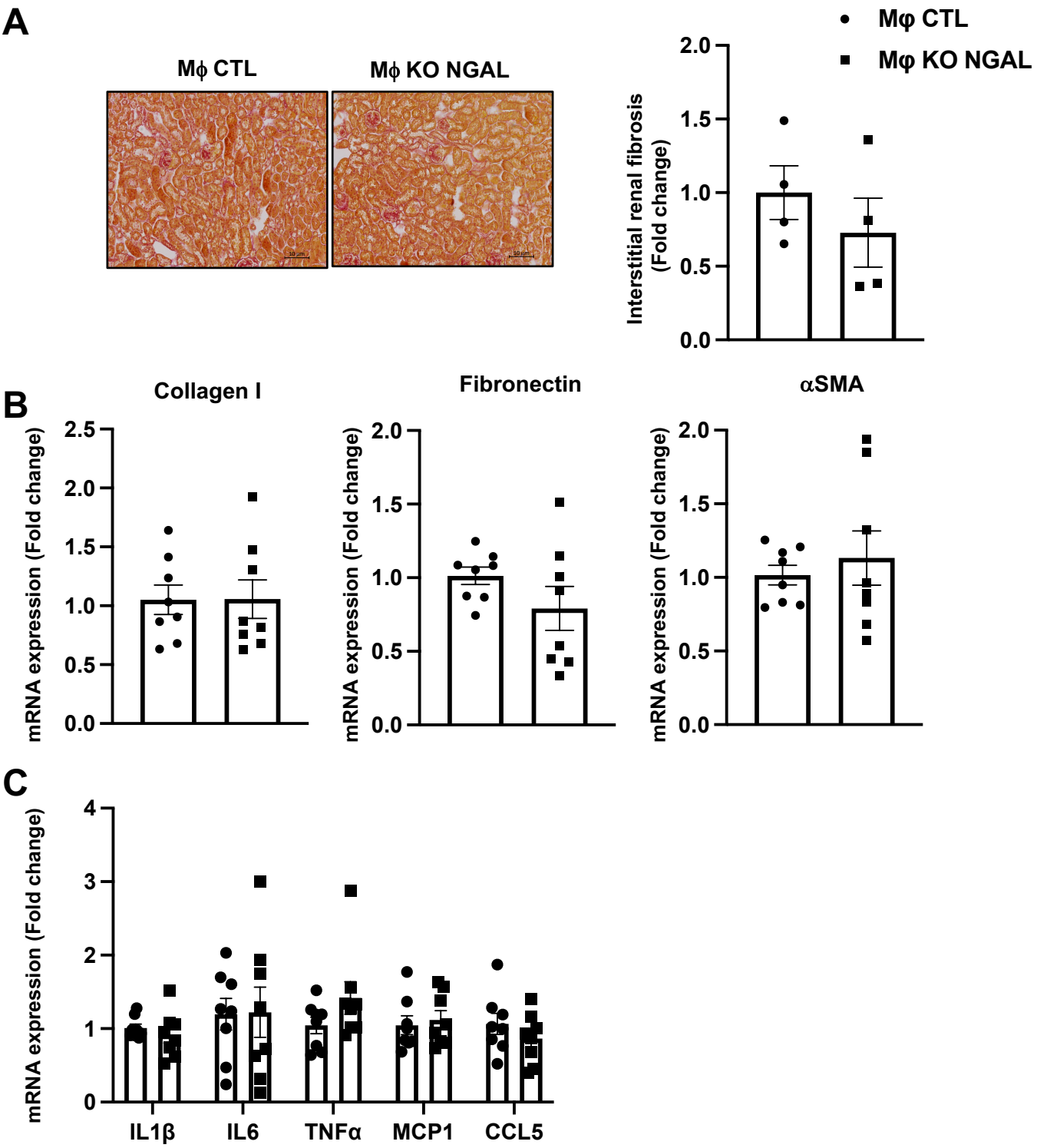

Figure S5. Renal phenotyping of untreated MΦ KO NGAL mice. **(A)** Representative images of Sirius Red staining with quantification**. (B)** mRNA expression of pro-fibrotic markers, such as collagen I, fibronectin, αSMA. **(C)** Gene expression of proinflammatory markers analyzed in whole kidney from MΦ CTL and MΦ KO NGAL mice. Student t-test was used for statistical analysis, n = 4-8. Scale bare 10 μm.

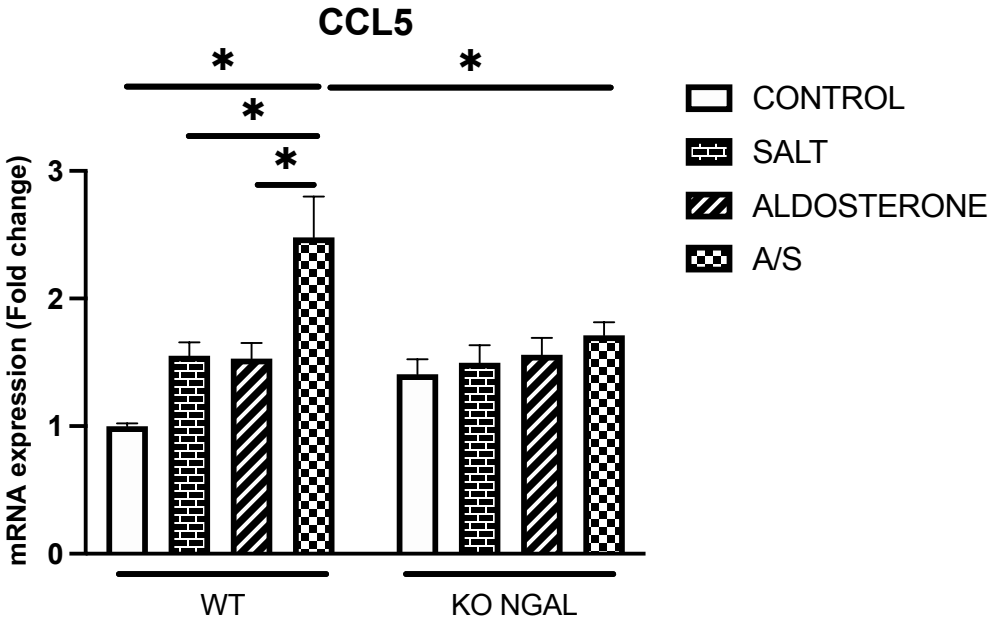

Figure S6. CCL5 mRNA expression in cultured MΦ from WT and KO NGAL mice treated by aldosterone or salt or by aldosterone and salt co-treatment . Aldosterone or salt alone treatment did not modify CCL5 gene expression in cultured WT MΦ while A/S combination had an additive effect. Two-way ANOVA was used for statistical analysis, $n = 5$. *$P < 0.05$.

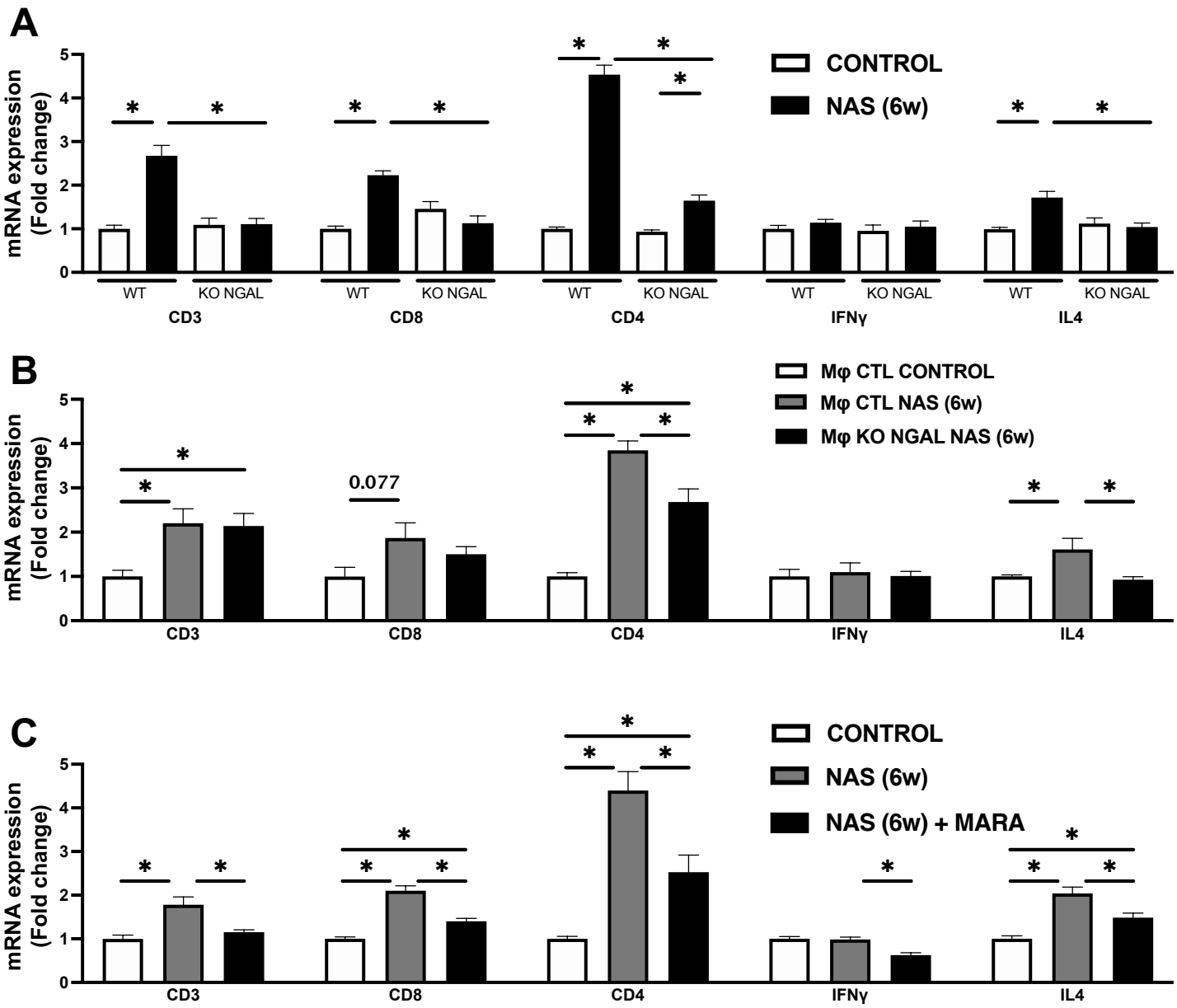

Figure S7. mRNA expression of T cells (*CD3*), cytotoxic T cells (CD8), T helper cells (CD4) markers and for interferon gamma (*IFNγ*) and interleukin 4 (*IL4*) in global KO NGAL model(**A**), specific KO NGAL in macrophage model (**B**) and mice treated with maraviroc (**C**). Two-way or One-way ANOVA were used for statistical analysis, n = 5-10. *P< 0.05

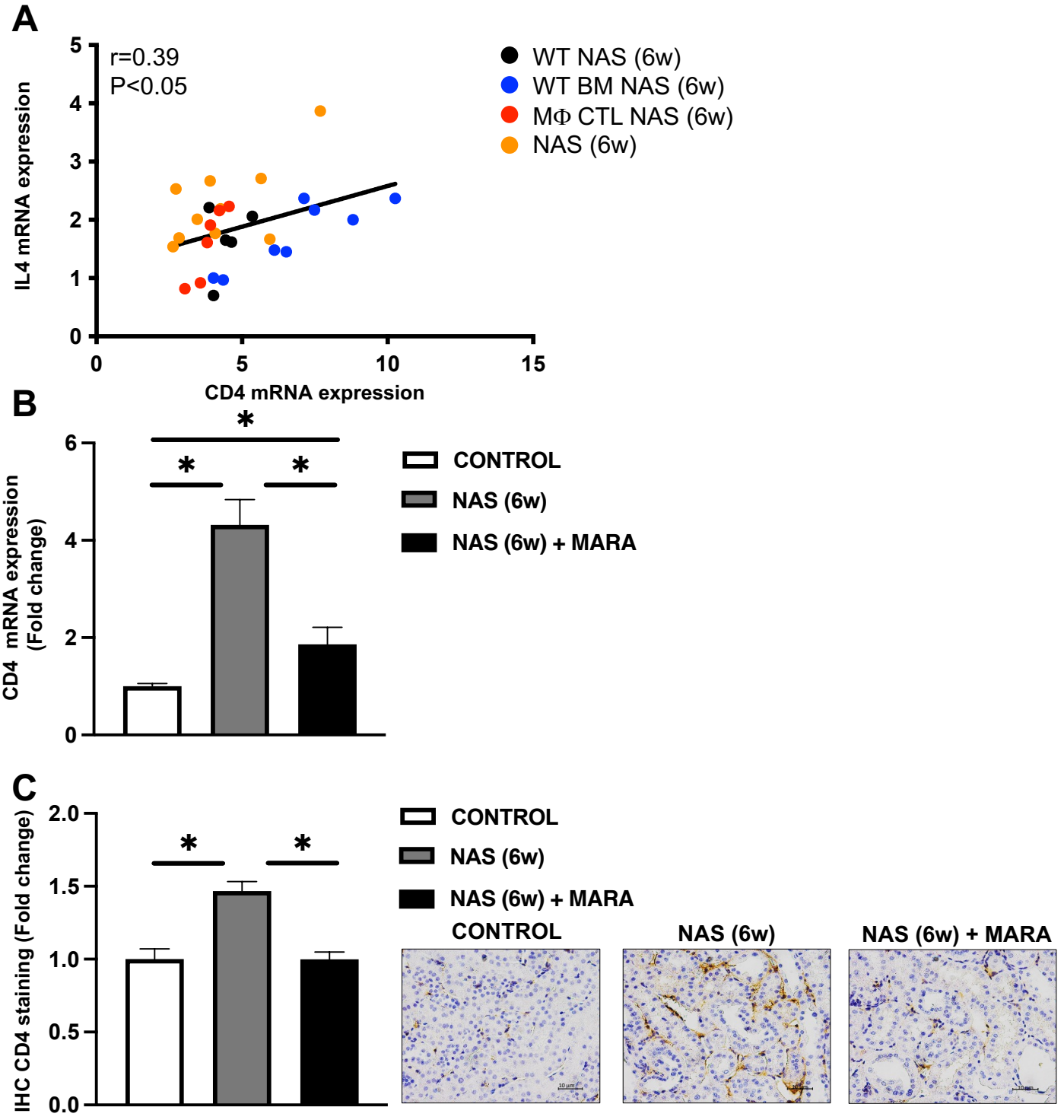

Figure S8. Correlative, mRNA and protein expression of CD4 in kidney. **(A)** Correlation between *IL4* and *CD4* expression in kidney from mice exposed to NAS challenge. A Pearson correlation test has been performed P < 0.05. **(B-C)** CD4 expression was analyzed by qPCR **(B)** and labelled immunostaining with quantification **(C)**. One-way ANOVA was used for statistical analysis, n = 7-10. *P< 0.05

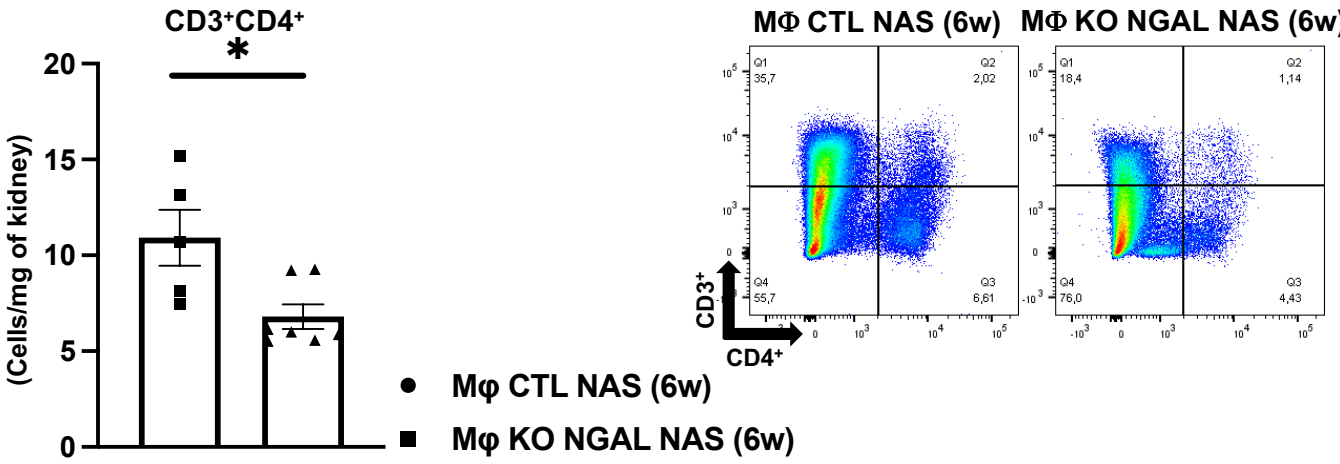

Figure S9. Analysis of $CD3^+CD4^+$ infiltration by FACS. Specific NGAL deletion in macrophages (MΦ KO NGAL) reduced $CD3^+CD4^+$ infiltration in kidney relative to control group (MΦ CTL) exposed to NAS challenge. Student t-test was used for statistical analysis, n = 5-7. *P< 0.05

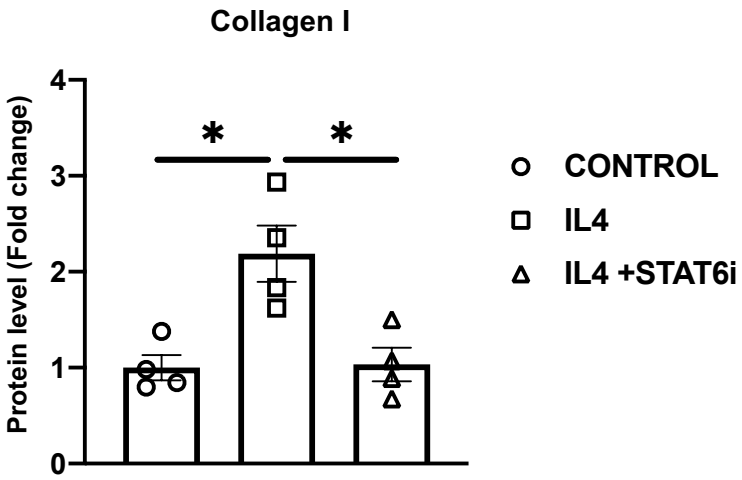

Figure S10. Increased of collagen I induced by IL4 in MKFs supernatant. Collagen I expression has been analyzed by ELISA. One-way ANOVA was used for statistical analysis, $n = 4$. *$P < 0.05$

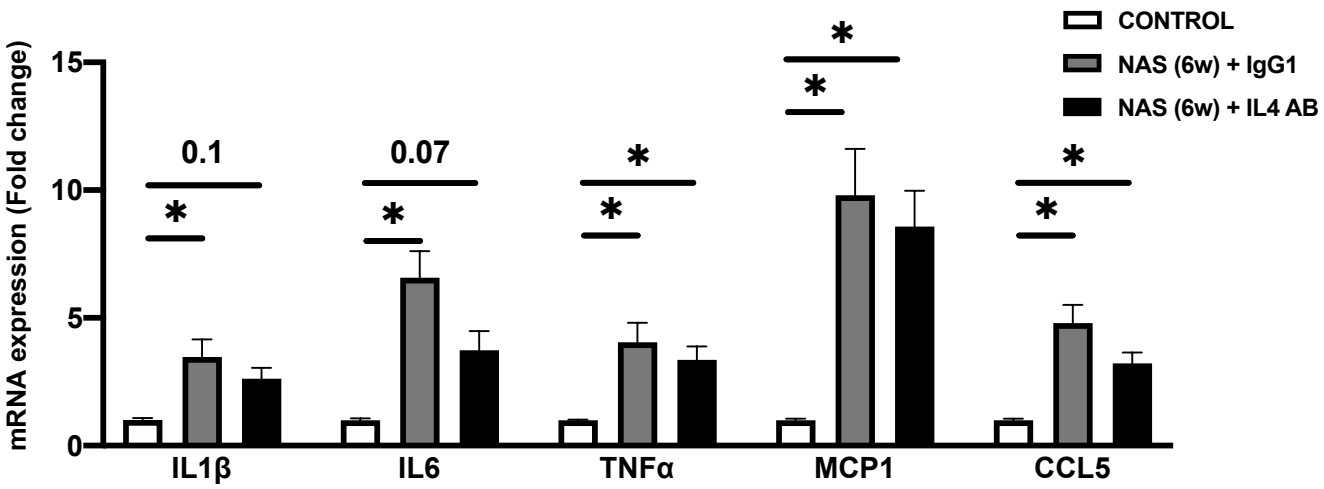

Figure S11. IL4 neutralizing did not improve renal inflammation induced by NAS. Gene expression of proinflammatory markers was analyzed by qPCR . One-way ANOVA was used for statistical analysis, n = 6-7. *P< 0.05

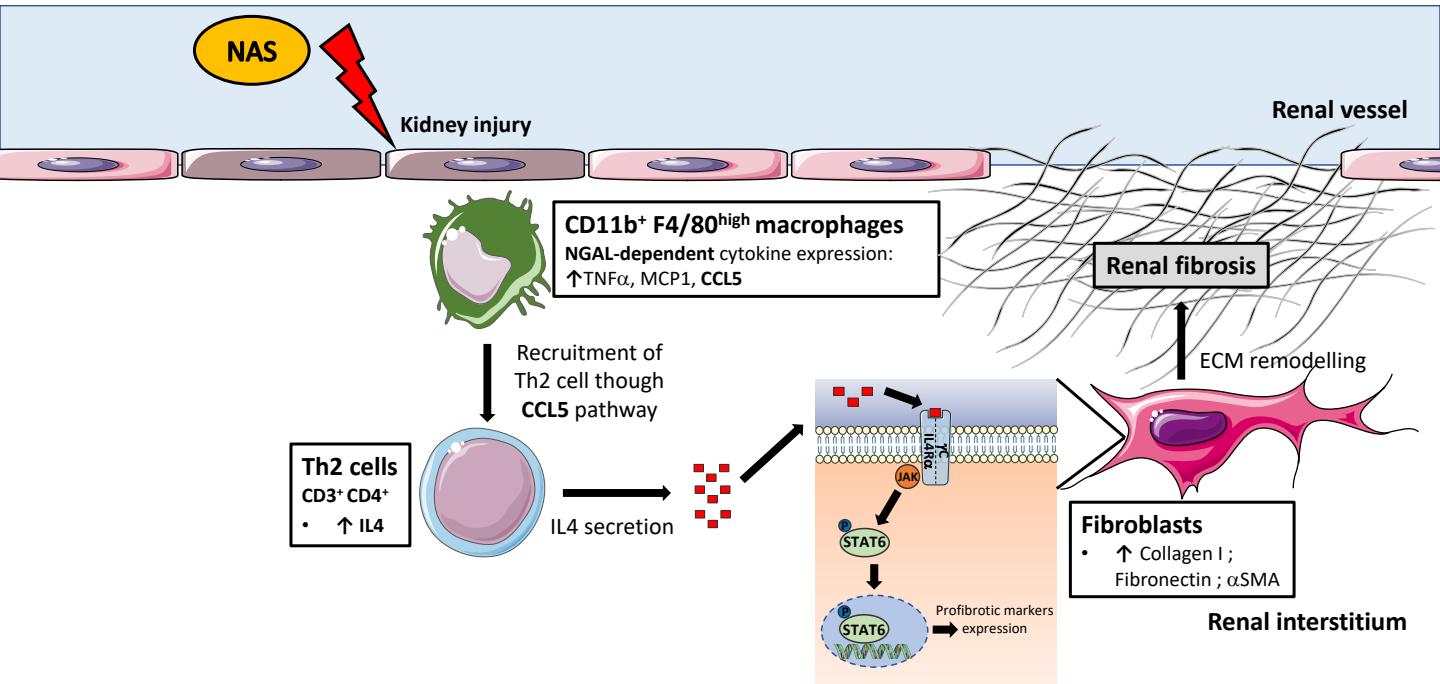

Figure S12. Determinant role of NGAL expressed in macrophages in NAS-induced renal fibrosis. Mineralocorticoid excess induces monocyte/macrophage infiltration into an inflamed area. In macrophages, NGAL is required for the expression of proinflammatory proteins like CCL5. Blockade of CCL5 signaling blunts renal Th2-cell recruitment and fibrosis induced by NAS challenge. The Th2-secreted cytokine IL4 has a direct profibrotic effect on kidney fibroblasts and may contribute to the development of renal fibrosis mediated by the aldosterone/NGAL/CCL5 signaling pathway.

Supplemental Tables

General characteristics	WT CONTROL	WT NAS	KO NGAL CONTROL	KO NGAL NAS
Body weight (g)	27.91±0.91	25.04±0.93*	30.40±0.35	27.41±0.44*
Kidney weight/Tibia Length (mg/mm)	8.95±0.44	18.25±1.38*	9.70±0.45	18.78±0.53*
Systolic Blood Pressure (mmHg)	117.2±2.01	132.3±4.60*	111.8±1.75	116.8±1.34†
Plasma Creatinine level (μM)	9.71±0.40	14.14±0.77*	8.44±0.62	11.17±0.46†

Table S1. Physiological parameters in KO NGAL mice exposed to NAS challenge.
Two-way was used for statistical analysis. n=5 *p<0.05 *vs* WT CONTROL. †p<0.05 *vs* WT NAS

Gene	q value	Fold change	Gene	q value	Fold change
Ager	0.7992	1.322	Cd163	0.0098	1.268
Alox12	0.7992	0.509	Cd4	0.7992	1.192
Alox15	**0.0040**	**1.497**	Cd40	0.0211	1.202
Alox5	0.0224	1.388	Cd40lg	0.0129	1.521
Areg	0.9948	1.024	Cd55	0.9948	0.987
Arg1	**0.0012**	**2.564**	**Cd86**	**0.0073**	**1.291**
Atf2	0.9948	1.045	Cdc42	0.8930	1.064
Bcl2l1	0.9948	1.027	Cebpb	0.0292	1.117
Bcl6	0.9948	0.985	Cfb	0.0001	2.330
Birc2	0.9948	0.961	Cfd	0.9948	1.283
C1qa	0.0270	1.154	Cfl1	0.9948	1.068
C1qb	0.9948	0.945	Chi3l3	0.9948	1.065
C1ra	0.0166	1.356	Creb1	0.9948	0.986
C1s	0.9002	0.814	Crp	0.9948	0.859
C2	0.0271	1.191	**Csf1**	**0.0030**	**1.890**
C3	**0.0040**	**1.592**	Csf2	0.9948	1.186
C3ar1	0.9948	1.015	Csf3	0.8651	1.629
C4a	0.0030	1.493	Cxcl1	0.9948	0.990
C6	0.9948	1.198	Cxcl10	0.9948	0.997
C7	0.9948	0.866	Cxcl2	0.9948	0.837
C8a	0.9948	1.236	Cxcl3	0.7992	0.524
C8b	0.7992	1.407	Cxcl5	0.8886	0.754
C9	0.7992	1.354	Cxcl9	0.9948	0.816
Ccl11	0.9948	0.900	Cxcr1	0.9948	1.163
Ccl17	**0.0030**	**1.605**	Cxcr2	0.9948	1.072
Ccl19	0.9948	1.014	Cxcr4	0.9948	0.953
Ccl2	0.0292	1.298	**Cysltr1**	**0.0073**	**1.293**
Ccl20	0.9948	1.003	Cysltr2	0.9948	1.024
Ccl21a	0.9002	1.214	Daxx	0.9948	0.998
Ccl22	0.9948	0.806	Ddit3	0.9948	0.970
Ccl24	**0.0085**	**1.831**	Defa-rs1	0.7992	1.317
Ccl3	0.9948	0.997	Elk1	0.9948	1.070
Ccl4	0.9948	0.979	Fasl	1.0000	1.001
Ccl5	**0.0085**	**1.366**	Flt1	0.9948	0.969
Ccl7	**0.0073**	**1.409**	Fos	0.0292	1.147
Ccl8	0.7992	0.625	Fxyd2	0.7992	0.723
Ccr1	**0.0030**	**1.415**	Gnaq	0.9948	0.991
Ccr2	0.9948	1.040	Gnas	0.9948	1.038
Ccr3	0.9948	0.935	Gnb1	0.9948	1.055
Ccr4	0.9948	1.010	Gngt1	0.9948	0.908
Ccr7	0.9948	0.814	Gpr44	0.9948	1.078
Grb2	0.9571	1.055	Il23r	0.9948	0.921

Gene	q value	Fold change	Gene	q value	Fold change
H2-Eb1	0.9948	0.913	Il4	0.9948	1.045
Hc	0.9948	0.948	Il5	0.9948	0.720
Hdac4	0.9948	0.947	Il6	0.7992	0.738
Hif1a	**0.0030**	**1.298**	Il6ra	0.9948	0.979
Hmgb1	0.9571	1.056	Il7	0.9948	0.988
Hmgb2	0.9948	0.858	Il9	0.7992	1.298
Hmgn1	0.9948	1.026	Irf1	0.9948	0.962
Hras1	0.7992	1.229	Irf3	0.9948	0.932
Hsh2d	0.9948	1.015	Irf5	0.9948	1.036
Hspb1	**0.0065**	**1.537**	**Irf7**	**0.0013**	**1.632**
Hspb2	0.9948	1.056	Itgb2	0.9948	1.012
Ifi27l2a	**0.0017**	**1.345**	Jun	0.7992	1.083
Ifi44	**0.0030**	**1.770**	Keap1	0.9948	1.020
Ifit1	**0.0073**	**1.404**	Kng1	0.9948	1.079
Ifit2	**0.0085**	**1.548**	Limk1	0.9948	0.965
Ifit3	**0.0034**	**1.456**	Lta	0.9948	1.027
Ifna1	0.7992	1.346	Ltb	0.9948	1.081
Ifnb1	0.9948	0.786	Ltb4r1	0.9948	0.914
Ifng	0.9948	1.109	Ltb4r2	0.9948	0.980
Iigp1	0.9948	1.048	Ly96	0.9948	0.970
Il10	0.9948	1.180	Maff	0.7992	0.934
Il10rb	0.7992	1.081	Mafg	0.9948	0.966
Il11	0.8618	0.763	Mafk	0.9948	1.041
Il12a	0.9948	0.772	Map2k1	0.7992	0.936
Il12b	0.9948	1.263	Map2k4	0.9948	0.996
Il13	0.9948	1.046	Map2k6	0.9948	0.950
Il15	0.9948	1.003	Map3k1	0.9948	1.022
Il17a	**0.0100**	**1.670**	Map3k5	0.0292	1.118
Il18	0.0168	1.151	Map3k7	0.9948	1.037
Il18rap	0.7992	0.830	Map3k9	0.9948	1.036
Il1a	0.9948	0.990	Mapk1	1.0000	0.999
Il1b	0.7992	0.433	Mapk14	0.9948	0.961
Il1r1	0.7992	0.769	Mapk3	0.9948	1.006
Il1rap	0.9948	1.011	Mapk8	0.9948	0.974
Il1rn	0.0292	1.144	Mapkapk2	0.9948	0.980
Il2	0.9948	1.051	Mapkapk5	0.9948	0.924
Il21	0.9948	1.004	Masp1	0.9948	0.929
Il22	0.9948	1.061	Masp2	0.9948	1.080
Il22ra2	0.9948	1.247	Max	0.9948	0.938
Il23a	0.9696	1.270	Mbl2	0.9948	1.187
Mef2a	0.9948	0.952	Raf1	0.9948	0.983
Mef2b	0.9948	1.078	Rapgef2	0.9948	0.958

Gene	q value	Fold change	Gene	q value	Fold change
Mef2d	0.0292	1.121	Relb	0.9696	0.933
Mknk1	0.9948	1.011	**Retnla**	**0.0000**	**2.180**
Mmp3	0.9948	0.987	Rhoa	0.9090	1.034
Mmp9	**0.0040**	**1.675**	Ripk1	0.9948	0.999
Mrc1	0.7992	1.146	Ripk2	0.9948	0.985
Mx1	0.0287	1.217	Rock2	0.9948	1.017
Mx2	0.9948	0.994	Rps6ka5	0.8930	1.099
Myc	0.9948	0.976	Shc1	0.9948	0.964
Myd88	0.9948	0.994	**Smad7**	**0.0022**	**1.402**
Myl2	0.9948	1.144	Stat1	0.0208	1.199
Nfatc3	0.9948	1.014	Stat2	0.7992	0.882
Nfe2l2	0.9948	1.030	Stat3	0.7992	0.887
Nfkb1	0.9948	1.014	Tbxa2r	0.9948	1.072
Nlrp3	**0.0073**	**1.321**	Tcf4	0.7992	0.918
Nod1	0.9948	0.943	Tgfb1	0.9948	0.971
Nod2	0.7992	0.812	Tgfb2	0.0236	1.115
Nos2	0.8930	0.832	Tgfb3	0.0270	1.367
Nox1	0.9948	1.126	Tgfbr1	0.7992	1.076
Nr3c1	0.9948	1.011	Tlr1	0.9948	1.074
Oas1a	0.7992	0.893	Tlr2	0.7992	0.873
Oas2	0.7992	0.806	Tlr3	0.9948	0.957
Oasl1	**0.0034**	**1.239**	Tlr4	0.9948	1.005
Pdgfa	0.0226	1.176	Tlr5	0.9948	0.959
Pik3c2g	0.9948	1.134	Tlr6	0.9948	1.048
Pla2g4a	0.7992	0.854	Tlr7	0.9948	0.955
Plcb1	**0.0073**	**1.199**	Tlr8	0.9948	0.985
Ppp1r12b	0.9948	0.944	Tlr9	0.9948	1.040
Prkca	0.9948	0.945	Tnf	0.9948	0.936
Prkcb	0.9948	1.021	Tnfaip3	0.7992	1.106
Ptger1	0.9948	1.010	Tnfsf14	0.9948	1.091
Ptger2	0.9948	0.973	Tollip	0.9948	1.020
Ptger3	0.9948	1.037	Tradd	0.9948	0.985
Ptger4	0.7992	0.917	Traf2	0.9948	0.996
Ptgfr	0.9948	0.855	Trem2	0.0308	1.048
Ptgir	0.9948	0.975	Tslp	0.9948	0.925
Ptgs1	0.0292	1.267	**Twist2**	**0.0030**	**1.264**
Ptgs2	**0.0030**	**1.871**	Tyrobp	0.9948	1.040
Ptk2	0.9948	0.990			
Rac1	0.9948	1.022			

Table S2. Detail gene expression from Nanostring analysis.

Fold change of gene expression compared WT MΦ + A/S vs KO NGAL MΦ + A/S groups. Genes in bold represent genes with a significative difference of expression between two groups. False discovery changes two-stage step-up method for Benjamini, Krieger and Yekutieli was performed for statistical analysis. $n = 5$. $q < 0.05$.